**TRIBHUVAN UNIVERSITY**

**INSTITUTE OF ENGINEERING**

**PULCHOWK CAMPUS**

**THESIS NO: M-372-MSREE-2019-2023**

**Viability Of Renewable Energy Extraction From Low Velocity Water Currents Using Vortex Induced Vibration Based Turbine**

**by**

**Sumesh Ghatane**

**A THESIS**

**SUBMITTED TO THE DEPARTMENT OF MECHANICAL AND AEROSPACE ENGINEERING IN PARTIAL FULFILLMENT OF THE REQUIREMENTS FOR THE DEGREE OF MASTER OF SCIENCE IN RENEWABLE ENERGY ENGINEERING**

**DEPARTMENT OF MECHANICAL AND AEROSPACE ENGINEERING**

**LALITPUR, NEPAL**

**OCTOBER, 2023**

# COPYRIGHT

# TRIBHUVAN UNIVERSITY

# INSTITUTE OF ENGINEERING

# PULCHOWK CAMPUS

# DEPARTMENT OF MECHANICAL AND AEROSPACE ENGINEERING

The undersigned certify that they have read, and recommended to the Institute of Engineering for acceptance, a dissertation entitled "VIABILITY OF RENEWABLE ENERGY EXTRACTION FROM LOW VELOCITY WATER CURRENTS USING VORTEX INDUCED VIBTATION BASED TURBINE" submitted by M.Sc. candidate in partial fulfillment of the requirements for the degree of Master of Science in Renewable Energy Engineering.

Supervisor:

Prof. Dr. Tri Ratna Bajracharya

Department of Mechanical and Aerospace Engineering

Institute of Engineering, Pulchowk Campus, Lalitpur

External Examiner:

Er. Anil Sapkota

Junior Professor

Nepal Engineering College, Bhaktapur

Committee Chairperson:

Asst. Prof. Dr. Sudip Bhattarai

Head of Department

Department of Mechanical and Aerospace Engineering

Institute of Engineering, Pulchowk Campus, Lalitpur

Date: October 4, 2023

# ABSTRACT

From the dawn of time, humans have been harnessing the kinetic energy of the flowing water bodies using various technologies. All those technologies require a decent flow velocity and discharge of the water bodies, otherwise it would fail to operate. However, the slow and steady motion of the earth's water bodies carries a vast majority of untapped energy resources. Whether it's a slow-moving ocean current or the flow of the rivers in plain basins, harnessing the kinetic energy from these low-velocity water bodies represents a promising avenue for the extraction of vast amounts of clean energy. There are various types of systems that have been designed and tested by researchers for extracting energy from slow-moving water bodies. While, this thesis focuses on using the vortex shedding phenomenon for energy extraction and investigates the potential of extracting renewable energy from low-velocity water currents using a Vortex-Induced Vibration (VIV)-based turbine system. Many marine turbines and energy extraction systems are in existence but due to the high cost of maintenance, they are proven unsuitable for real-world application. The strong point of using VIV-based turbines for underwater applications is their simplicity of construction, low cost, and low maintenance design. By relying on the VIV phenomenon, these turbines offer an innovative solution to generate electricity without the need for high flow rates typically associated with conventional hydroelectric systems. This system offers a promising solution to meet the growing global demand for scalable renewable energy sources as well. Additionally, these Vortex-Induced Vibration turbines can be employed in conjunction with conventional turbines at the outlet section where the flow velocity has been drastically reduced, allowing for the capture of residual energy at the output stage while increasing the overall efficiency of the system. To support the increasing energy demand while minimizing ecological intrusion, new technologies are required and VIV-based energy extraction presents one of the promising solutions to the existing problems. The kinetic energy harvested by this turbine will be converted to electrical energy from a suitable power takeoff mechanism, which can be further utilized for various applications. The energy produced is cent percent safer, clean, and more important, sustainable.

# ACKNOWLEDGEMENT

# TABLE OF CONTENTS

# LIST OF TABLES

# LIST OF FIGURES

## LIST OF SYMBOLS

| | |
|---|---|
| *F* | Force |
| $\delta$ | Deflection |
| $Q_{max}$ | Maximum discharge of fluid |
| $R_e$ | Reynolds Number |
| $F_s$ | Vortex shedding Frequency |
| S | Strouhal Number |
| u | Velocity |
| $u_u$ | Velocity in x-axis |
| $u_v$ | Velocity in y-axis |
| $u_w$ | Velocity in z-axis |
| $\upsilon$ | kinematic viscosity |
| J | joules |
| N | Newton |
| W | Watt |
| Hz | Hertz |
| mm | Millimeter |
| cm | Centimeter |
| m | Meter |

# LIST OF ACRONYMS AND ABBREVIATIONS

CFD             Computational Flow Dynamics

CAD             Computed Aided Drawing

VIV             Vortex Induced Vibration

2-D             Two dimensional

3-D             Three dimensional

PVC             Poly Vinyl Chloride

# CHAPTER ONE: INTRODUCTION

## 1.1 Background

Energy is the driving force of the nature and our modern society. As the society is evolving the demand for energy is increasing day after day. The energy system today depends on fossil fuels as its major part and everyone is aware that its supply is limited and very soon it will be empty. Population is increasing and the technology is evolving and the both have a common demand i.e., more and more energy.

We know from our experience that any of the non-renewable sources of energy, whether it is fossil fuel, nuclear energy etc. any energy intensive but are non-replenishable and are non-sustainable. Furthermore, they leave out byproducts that are hard to dispose and it causes serious threats to the biosphere. Since, the industrial age we have released a staggering 37.12 billion metric tons up to 2021 (Ian Tiseo,2023) of Carbon dioxide gas into atmosphere. Hence, we see that our energy trend should change from traditional to a more ecofriendly alternative.
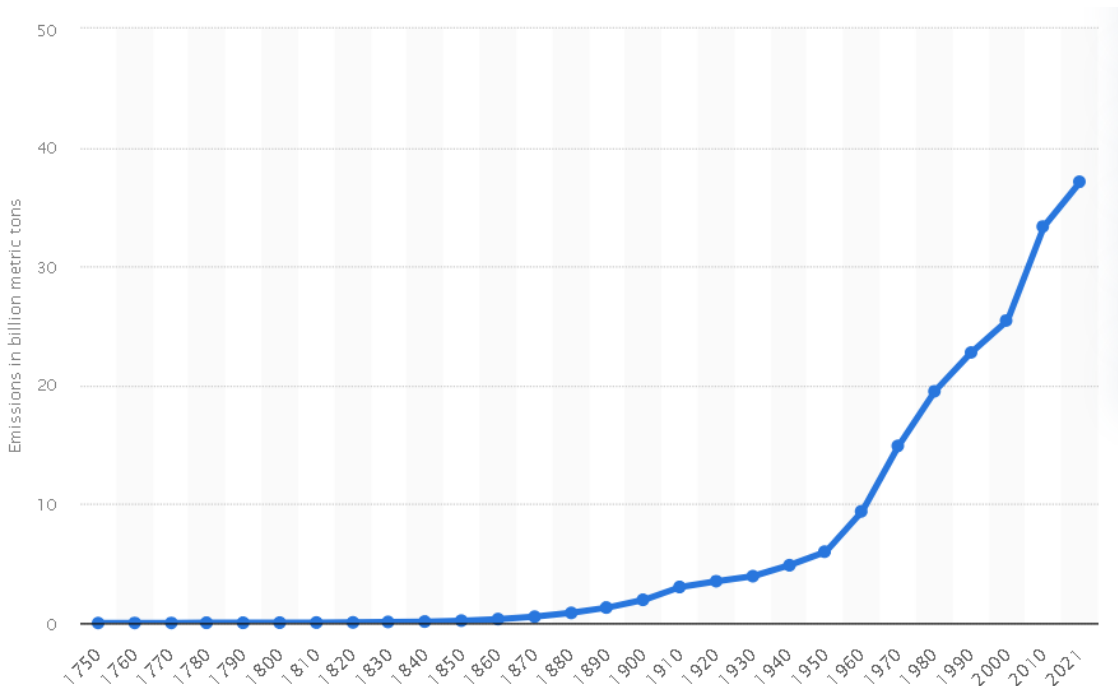


Figure 1.1 Historical carbon dioxide emissions from global fossil fuel combustion and industrial processes from 1750 to 2021 [Ian Tiseo,2023]

Renewable sources of energy comprise of energy sources which can be renewed and reused again and again without worrying about their depletion or their consequences. They are more ecofriendly and their sustainability is excellent. Solar energy, wind energy, tidal energy etc. fall on this category. It has many advantages over the traditional energy source but its major cons are its availability and intermittence nature.

There are many sources of renewable energy explored but only a few solutions are commercially exploited. It's a well-known fact that 3/4th of the earth's surface is covered by ocean and water bodies. An estimated 3.04 x $10^{21}$ joules of energy are available in the ocean alone (Bobby Zarubin, 2015) and the total primary energy consumption of the world in 2021 was 5.9515 x $10^{20}$ joules (bp, 2022). As there is a huge supply of energy in the ocean and slow flowing water currents that, if tapped, can fulfil every day energy requirements of the whole world with clean renewable energy. The potential of
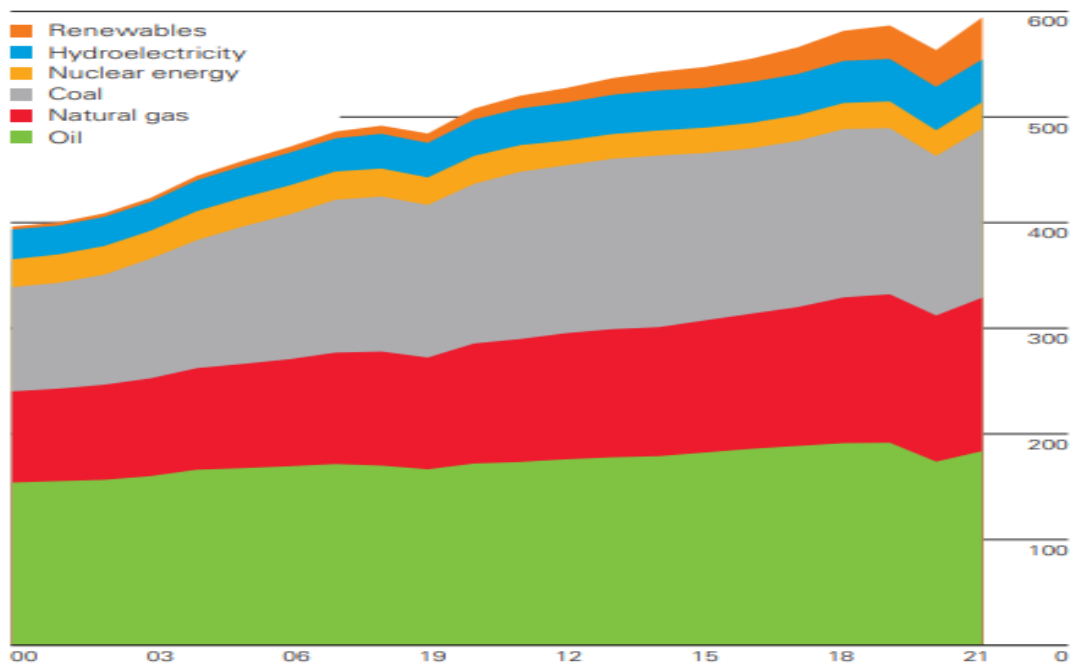


Figure 1.2 : World energy consumption (2021) [bp, 2022]

harnessing energy from vortex-induced vibrations (VIV) from marine currents and slow flowing water bodies to extract energy offers a promising solution to meet the growing global demand for scalable renewable energy sources. While current hydrokinetic energy technologies exist, they have limitations that hinder their ability to fully satisfy this demand. Exploiting the slow and steady motion of Earth's water bodies represents a vast and untapped energy resource. Traditional energy generation from water flow involves the joint effort of a dam and a hydroelectric generator, which can have ecological and

environmental impacts. To support the increasing energy demand while minimizing ecological intrusion, new technologies are required. VIV-based energy extraction presents a promising solution. Typically, structures exposed to fluid flow are designed to minimize fatigue caused by vortex-induced vibrations. However, recent developments propose enhancing these vibrations to maximize energy extraction. The technology involves securing a cylinder horizontally or vertically in water and constraining its motion to a single degree of freedom- in the plane perpendicular to the fluid flow. As fluid flows over the cylinder, an alternating vortex pattern is created, exerting lift forces that push the cylinder up and down or sideways. This motion is then converted into electricity using a power take-off mechanism. Compared to traditional hydro technology, VIV-based generators offer several advantages. Most turbine-based converters operate efficiently only at currents exceeding 2 m/s (S. M. Ingole, Dr. S. S. Patil, 2021), while surface oscillation converters have limited high-output ranges of wave frequencies. In contrast, VIV-based technology has the potential to operate efficiently in slow-moving waterways across a wide range of frequencies. Additionally, large-scale tidal and dam systems are capital-intensive and environmentally intrusive, whereas VIV-based technology can generate energy from water flow without altering the local environment, posing dangers to nearby residents, changing the landscape visibly, or interfering with water traffic in slow-moving waterways. Coastal areas also present significant potential for energy generation through VIV.

## 1.2 Problem Statement

There is a vast amount of energy contained in the slow flowing water and ocean currents. There is a huge domain of energy which has a huge potential of energy. Most of the turbines operates at a greater flow velocity but very few approach has been made to harness the energy available in them.

UN Sustainable Development Summit held in New York on September 2015 introduced 17 sustainable goals, where goal 7 (SDG7) is about ensuring access to clean and affordable energy by 2030. SDG7 includes the following goals;

   i.   universal access to affordable, reliable and modern energy services,
   ii.  increasing substantially the share of renewable energy in the global energy mix
   iii. doubling the global rate of improvement in energy efficiency.

As there is a huge supply of energy in the ocean and slow-moving water currents that, if tapped, can fulfill every day energy requirements of the whole world with clean renewable energy. There have been many projects done in order to harness the energy available in the ocean, but because of various reasons not as much of the potential energy have been unlocked. One of the main reasons is the high cost of maintenance.

On the other hand, non-renewable energy sources like fossil and nuclear energy are diminishing day after day and the rise of the consciousness of the modern world to conquer clean and sustainable green energy to fulfill the demand of the current energy market is to the fullest. Hence, a viable solution needs to be made to cut the trend and break the traditional trends. Also, many limitations need to be addressed for ocean and slow-moving water current energy extraction to be used successfully at a commercial scale. Some of the engineering and technical challenges that needs to be addressed includes the following:

i. Avoidance of cavitations (bubble formation)
ii. Prevention of marine growth buildup
iii. High maintenance costs
iv. Corrosion resistance
v. Generation of electromagnetic fields (EMF)
vi. Toxicity of paints, lubricants, and antifouling coatings
vii. Interference with animal movements and migrations, including entanglement and strike by rotor blades or other moving parts

## 1.3 Objectives

**Main Objective**

The main objective of this thesis is:

- To study the viability of Vortex Induced Vibration turbine also known as Bladeless turbine for renewable energy extraction from slow flowing water currents using model of turbine.

**Specific Objective**

- To create a CAD design of a VIV turbine.
- To perform simulation using CFD software and record as well as analyze data.
- To design and fabricate and perform experiments on the model of VIV turbine and verify its experimental results.

- To conclude the study of the viability of VIV turbine to extract renewable energy from slow flowing water current.

## 1.4 Rationale

The world is evolving and the demand for cleaner and sustainable energy is at upmost for driving the society. The energy generation must be more affordable, cleaner and most importantly sustainable. There are various technologies used for the extraction of clean energy from renewable sources and they are in operation too. An additional supply of energy is required to fulfill the demand for energy today and it may come from a rather unusual source i.e., the slow flowing water currents. VIV induced vibration-based energy extraction method meets the requirement for extracting clean energy from slow flowing marine or any aquatic currents. It has a simple design and fewer moving parts making it cheaper and has a very low maintenance frequency. This makes it excellent choice for under water application.

## 1.5 Assumption

- The CFD simulation is done with ideal uniform laminar flow condition.
- The simulation may lack some real-world variables like intermittence nature of water current etc.
- The displacement of model is calculated using small angle approximation.
- The buoyant force was neglected.

## 1.6 Outline of the Report

This report has been divided into four chapters. A brief outline of each chapter is given below.

- **Chapter 1:** It gives background of the problem associated with renewable energy extraction for low velocity water and marine currents. It discusses about the problem statement, rationale and objective of the report.
- **Chapter 2:** This chapter gives summary of research work done in area of Vortex Induced Vibration based Turbine and energy extraction from low velocity marine and water currents in different books, journals, etc.
- **Chapter 3:** This chapter elaborates about the research methodology involved in performing the research. It includes everything from experimental setup, instrumentation method, data collection method and detailing about the research to be

5

performed. It also elaborates about fabrication method, location, model generation along with the computational fluid dynamics method and simulation.

- **Chapter 4:** This chapter discusses the results obtained from the experiment and simulation. The simulation result was verified with the experimental results.

- **Chapter 5:** This chapter gives the overall conclusion of the research. Based on the research recommendations and future scope for the research have been also mentioned in this chapter.

# CHAPTER TWO: LITERATURE REVIEW

## 2.1 Vortex Shedding

Vortex shedding is a commonly observed occurrence when a non-streamlined object, referred to as a bluff body, is immersed in a flowing fluid. In the presence of fluid viscosity, the flow establishes a boundary layer, which triggers the separation of this boundary layer along the body's surface, a process influenced by the body's shape. This separation creates a distinct layer that demarcates the wake from the undisturbed free-flowing stream, inducing rotational motion within the fluid. This rotation subsequently initiates the generation of vortices, which are expelled from the rear of the body and propagate downstream, producing a regular pattern recognized as a vortex street. (Bearman, 1984):

When vortices are shed asymmetrically, an uneven pressure distribution forms on both the upper and lower surfaces of the object, resulting in a net lift force perpendicular to the flow direction. Because vortex shedding happens periodically, these lift forces undergo cyclic variations, causing oscillatory motion. This phenomenon is recognized as vortex-induced vibration (VIV). In instances where the shedding frequency ($f_S$) closely aligns with the natural frequency of the moving object ($f_N$), a phenomenon called "lock-in" can manifest (Zhang, W., Li, X., Ye, Z., & Jiang, Y., 2015). Lock-in entails the adjustment of the shedding frequency to match the object's natural frequency, leading to heightened vibration amplitudes. This synchronization concern is of particular significance to structural engineers, as it can pose a risk of structural damage or failure.

The investigation of the shedding frequency range where lock-in can manifest is a pivotal aspect of vortex-induced vibration (VIV) research. This knowledge holds significance in the context of devising energy-harvesting systems. Despite its widespread recognition, VIV remains a complex and insufficiently understood phenomenon. Historical records dating as far back as the 15th century document early observations of vortex shedding. In modern times, extensive research efforts have been dedicated to examining the dynamics of vortex shedding and the variables that influence the movement of objects during VIV. While a substantial portion of research has concentrated on suppressing vortex shedding and alleviating VIV effects, comprehending VIV is equally vital for optimizing energy extraction capabilities.

Numerous engineered structures exposed to consistent fluid flows can exhibit vulnerability to vortex-induced vibration (VIV). Examples encompass offshore installations, marine risers, heat exchange apparatus, mooring cables, bridges, civil infrastructure, nuclear reactor components, and cooling stacks. VIV considerations are integral to the design phase in these domains. Although the predominant focus in prior research has been on suppressing VIV, the insights garnered from these investigations retain their relevance in comprehending this phenomenon. This knowledge also bears significance in the context of energy generation endeavors, where enhancing VIV effects is a desired outcome. It's important to note that much of the research surrounding VIV remains grounded in experimentation and empirical observations, offering practical guidelines rather than analytical models for the design process.
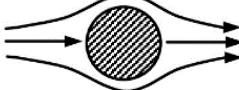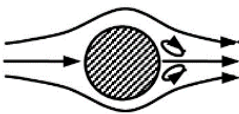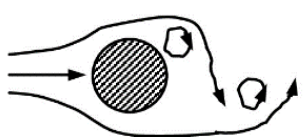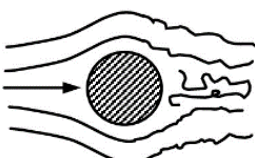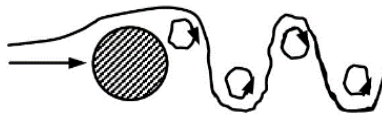
| | | |
|---|---|---|
| | $Re < 5$ | **Regime of unseparated flow** |
| | $5 \leq Re < 40$ | **A fixed pair of vortices in wake** |
| | $40 \leq Re < 90$ | **Vortex street is laminar** |
| | $90 \leq Re < 150$ | **Vortex street is laminar** |
| | $150 \leq Re < 300$ | **Transition range to turbulence in vortex** |
| | $300 \leq Re < 3(10^5)$ | **Vortex street is fully turbulent** |
| | $3(10^5) \leq Re < 3.5(10^6)$ | **Laminar boundary layer has undergone turbulent transition and wake is narrower and disorganized** |
| | $3.5(10^6) \leq Re$ | **Reestablishment of turbulent vortex street** |

Figure 3.1: Different Vortex shedding regimes (Mawat, 2018).

## 2.2 Vortex Induced Vibration

Vortex-induced vibration (VIV) is a widely acknowledged fluid dynamic phenomenon that has undergone comprehensive examination across diverse engineering domains. (Williamson, Charles HK, and R. Govardhan, 2004). Historically, VIV has been a point of concern in areas like offshore engineering and structural dynamics, predominantly viewed as a challenge to be minimized due to its potential to induce fatigue and structural wear. Nonetheless, researchers have identified the prospect of utilizing VIV as a method for generating electrical power from sluggish marine currents. This innovative concept revolves around capitalizing on the inherent interplay between fluids and structures during VIV to transform the mechanical energy produced by oscillating structures into electrical power. In recent times, there has been an escalating interest in investigating the viability of energy generation systems rooted in VIV, particularly within the context of renewable energy sourced from oceanic currents. By deploying specially crafted underwater turbines or oscillating cylinders, the VIV phenomenon can be harnessed to extract energy from the flow of slow-moving marine currents.

VIV-based turbine operates on a fundamental principle: as slow flowing water or ocean currents flow past these structures, they induce periodic vortex shedding, leading to the vibration or oscillation of the structures. The mechanical motion resulting from VIV can then be transformed into electrical energy through diverse mechanisms, including piezoelectric materials, electromagnetic induction, or specialized devices like fluidic diodes and arc-shaped generators. The key advantage of harnessing VIV for energy generation lies in its capability to tap into low-velocity marine currents, which may not be suitable for conventional turbine-based systems. This expands the range of potential deployment locations for marine energy projects, encompassing regions with slower current speeds or more irregular flow patterns.

Despite the promise of VIV-based energy generation, there are several technical hurdles that must be overcome for practical implementation. These challenges encompass optimizing the design of energy conversion systems to enhance efficiency and reliability, developing materials resilient enough to withstand harsh aquatic and marine environments, and addressing issues such as fatigue and corrosion. Nonetheless, ongoing research and development endeavors persist in this field, with numerous studies and pilot projects exploring the feasibility and performance of VIV-based hydro generators. By leveraging the VIV phenomenon, there exists the potential to harness a hitherto untapped

source of renewable energy, contributing to a more sustainable and diversified energy portfolio.

Nevertheless, it's essential to emphasize that the real-world application and effectiveness of such a system would hinge on a multitude of variables. These encompass the precise design and performance attributes of the VIV generators, the presence and intensity of water and ocean currents and the comprehensive economic viability of the system. While the concept presents potential, it necessitates additional research, development, and practical trials to ascertain the actual capacity and practicability of renewable energy extraction through the utilization of a cluster of VIV generators fine-tuned for low velocity water and oceanic currents.

## 2.3 Strouhal Number

A supplementary dimensionless factor has been introduced to establish a connection between the frequency of vortex shedding ($f_s$) and the prevailing flow conditions. This factor is denoted as the Strouhal number ($S$) and is defined in the equation provided below: (Watkins, S. ,2010).

$$S = \frac{f_s D}{U} \tag{1}$$

Where,

    $U$ = free stream velocity (m/s)

    $D$ = cylinder diameter (m)

    $f_s$ = Vortex shedding frequency (Hz)

Across a broad spectrum of Reynolds numbers, the Strouhal number exhibits minimal variation and can effectively be treated as a constant.

In the Reynolds number range of roughly $300 < Re < 10^5$, the Strouhal number (St) exhibits a consistent value of approximately 0.2 for smooth surfaces, closely matching the fully developed turbulent vortex street previously discussed. During experimental phases, the Reynolds number tends to fall within the middle of this stable Strouhal number range. Consequently, in experimental computations, the Strouhal number can be regarded as a constant, simplifying the determination of shedding frequency ($fs$), which now relies solely on the flow velocity ($U$) for a cylinder of a specified diameter.

For the given test setup, the anticipated shedding frequencies fall within the interval of *fs* = 0.8-2.0 s$^{-1}$, corresponding to flow velocities spanning from 0.15 to 0.30 m/s. These figures offer a projection of the shedding frequency tailored to the particular flow conditions and dimensions of the experimental apparatus.
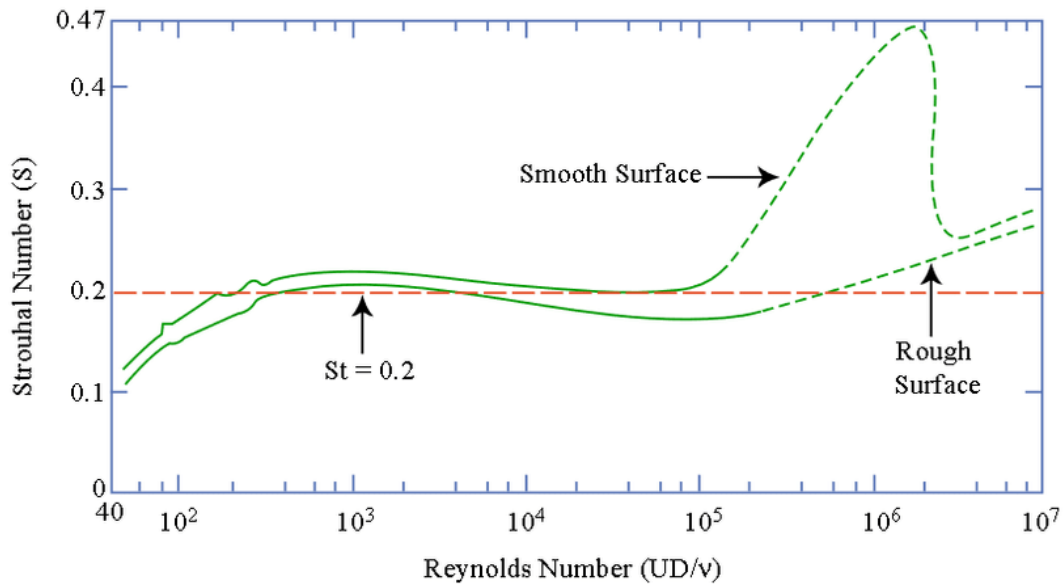


Figure 3.2: The correlation between the Strouhal Number and Reynolds Number for vortex shedding in a uniform stream. *Lienhard (1966) and Achenbach and Heinecke (1981)*

## 2.4 Principle of Vortex Induced Vibration Turbine

Mechanical energy can be derived from the kinetic energy of water currents through the utilization of a turbine. The functionality of the Vortex Induced Vibration Turbine or commonly referred as bladeless turbine relies on vortex induced vibration principle and resonance, enabling the transmission of energy to its structure by harnessing the hydro force through this phenomenon.

The device comprises a cylinder designed to oscillate upon water current impact, driven by the swirls or vortices created during the collision. This oscillatory motion, known as Vortex Induced Vibration (VIV), generates mechanical energy. Subsequently, an alternator converts this mechanical energy into electrical power. The cylinder is securely anchored to the ground through a supporting rod, with the upper section of the rod also providing support for the mast.

One of the primary advantages of this system is the elimination of mechanical components susceptible to wear from friction, leading to reduced maintenance costs and

11

an extended operational lifespan. Moreover, the absence of lubricants eliminates the need for managing potential waste associated with lubrication.

Another notable benefit of this technology is its significant reduction in environmental impact. While traditional hydro farm installations undergo a rigorous assessment of their environmental footprint, particularly in relation to aquatic life. In contrast, bladeless turbines exhibit far less movement, making it easier for animals to avoid them. Furthermore, their operation generates considerably less noise, reducing noise pollution.

Additionally, bladeless turbines require significantly less land compared to their traditional counterparts. Furthermore, these bladeless turbines exhibit faster adaptability to changes in water current direction, a valuable feature.

The benefit of employing a vortex indued vibration-based turbine lies in its capability to induce vibrations at resonance across a wide spectrum of Reynolds numbers, as indicated by the upper branch in the amplitude-velocity plots for flow over a cylinder.

# CHAPTER THREE: RESEARCH METHODOLOGY

This chapter provides an overview of the methodology employed throughout the project, spanning from its inception to its conclusion. It delves into the theoretical underpinnings of heat and mass transfer within a single-slope solar still and expounds on the computational aspects. Additionally, it offers a concise exploration of the various numerical techniques applicable for solving numerical problems. Furthermore, the chapter furnishes details about the experimental setups, analytical tools, materials employed, and the CAD geometry used in the study.

## 3.1 Theoretical framework

The research methodology is structured into distinct stages to comprehensively address various aspects of the study. Initially, a preliminary investigation is conducted to uncover the fundamental mechanisms and significant variables that influence the productivity of VIV turbine. This is followed by a critical step, where existing relationships and principles associated with bladeless turbine are theoretically determined through an in-depth analysis of various studies and literature reviews.

Concurrently, a conceptual or modified design is developed in parallel with the literature review to enhance the functionality and performance of the turbine. Subsequently, empirical testing is undertaken to identify and establish relationships among key parameters, providing valuable real-world insights.

To further advance the research, a theoretical model is crafted. This model comprehensively addresses theoretical values, as well as the vortex shedding phenomena within the turbine. It takes into account the influence of significant variables on the system's productivity, all rooted in fundamental engineering principles.

The research plan is thoughtfully organized into six phases, each encompassing specific functional elements and decisions. These phases serve as a structured guide, ensuring a methodical and effective progression of the research.

- Phase I: Preceding Research and Background Study
- Phase II: Verification of Conceptual Design
- Phase III: Experimental Testing
- Phase IV: CFD Modeling and Simulation
- Phase V: Model Verification and Validation
- Phase VI: Preparation of Thesis and Presentation

### 3.1.1 Phase I: Preceding Research and Background Study

The initial phase of the research encompassed the development of a foundational model based on the insights gathered from the literature review. Formulating this fundamental model was essential in order to acquire insights into the experimental design, necessary instrumentation, and the modeling process. Figure 3.1 illustrates this first phase, accompanied by a detailed explanation.
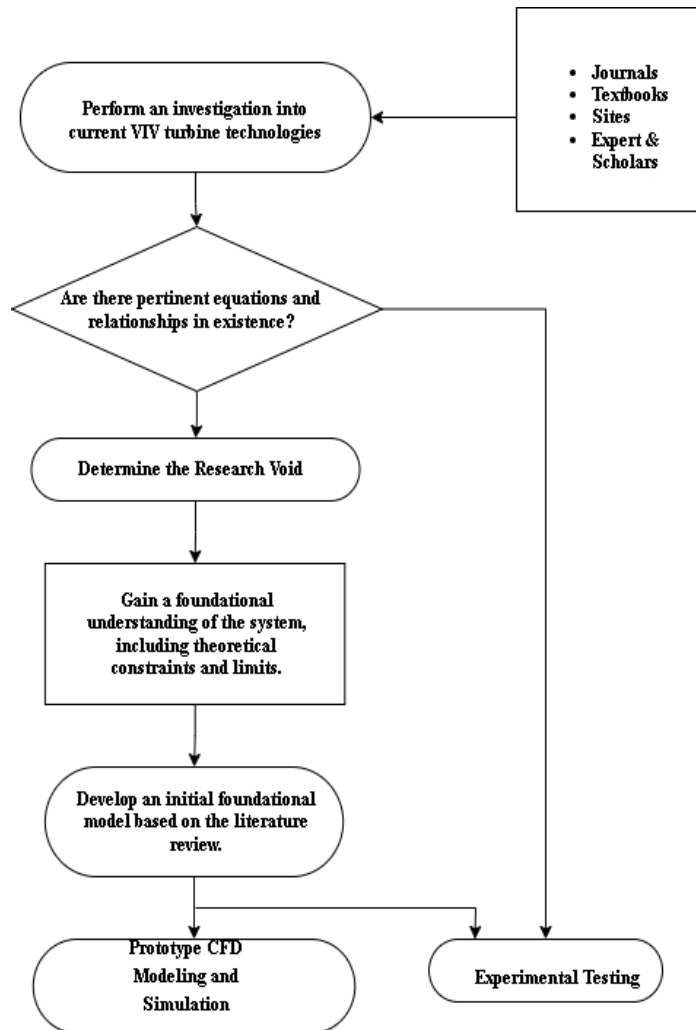


Figure 4.1: Flowchart of phase 1

### Phase I - A

Extensive literature was reviewed and analyzed concerning various VIV based energy extraction methods. This comprehensive study aided in the identification of crucial design elements, laying the groundwork for deriving key relationships. It also provided insights into which variables and aspects of the existing design warrant additional investigation through experimental testing and simulation. Additionally, the literature survey revealed

a spectrum of alternative techniques and current methods, enriching the understanding of VIV bladeless turbines.

**Phase I -B**

The presence of governing equations and relationships among key elements was established, forming the basis for identifying research gaps. In cases where no existing relationships were found, the research progressed directly to the experimental phase to establish these connections. A multitude of equations and relationships sourced from the literature were employed to gather data, thereby enhancing the understanding of previous research efforts.

If a specific design problem had not been previously addressed, gaps were pinpointed. Subsequently, the research was dedicated to bridging these recognized research gaps.

**Phase I -C**

At this stage, the culmination was an assessment of the collective knowledge in VIV energy extraction methods. This investigation served to validate the existing limits and boundary conditions, offering guidance for subsequent empirical testing.

**Phase I -D**

The result of this stage yielded the preliminary formulation of a power output from the model of VIV turbine. By integrating key elements identified through the literature review with fundamental principles, an initial model was established. The outcomes of this phase laid the foundation for the subsequent model development in Phase-IV and provided valuable insights into the required instrumentation and testing procedures.

### 3.1.2   Phase II: Verification of Conceptual Design

The second phase of the research aimed to validate the commercial relevance of the study.

**Phase II -A**

The design's functional elements were identified, and the mechanisms were validated. This stage involved meetings and discussions with the supervisor regarding the functionality, particularly in the event of design modifications.

**Phase II -B**

Several critical factors were taken into account to ensure the functionality of the design, encompassing unit size, suitability, construction feasibility, maintenance requirements,

and seamless integration with other units. Ultimately, this phase culminated in a clear and comprehensive assessment of the modified concept and design.

### 3.1.3 Phase III: Experimental Testing

The third stage of the research involved the development and construction of an experimental setup, along with the specification of necessary instrumentation for data collection. This process aimed to acquire the essential data needed to comprehend the behavioral patterns of various parameters under investigation. The details of this level are depicted in Figure 3.2 and further elucidated below.
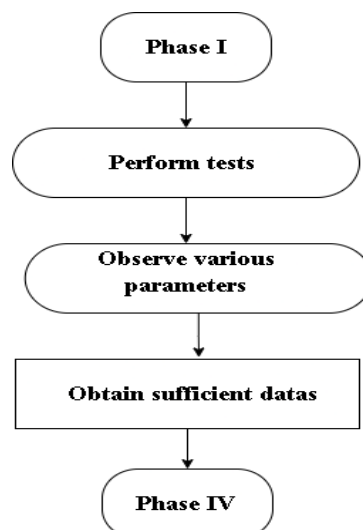


Figure 4.2: Flowchart of phase II

**Phase III -A**

The initial research phase centered on establishing relationships among critical operational, design, and other parameters. Experiments were conducted to assess the impact of these parameters, necessitating the development of an experimental setup. Additionally, a Prototype model and test tank was fabricated to facilitate the testing process. Moreover, a test was conducted on a actual river stream to find out the effectiveness of the model.

**Phase III -B**

The primary outcomes of the initial testing were the determination of the significant effects of the identified parameters. Among these parameters, a critical one was identified as having a substantial influence on the power extraction.

**Phase III -C**

Upon identifying the most critical parameter influencing power extraction from VIV turbine, an ample amount of relevant data was gathered through testing. This data will be instrumental in constructing the theoretical system model in Phase IV.

### 3.1.4   Phase IV: CFD Modeling and Simulation

The fourth research stage entailed the fusion of theoretical and empirical knowledge to create a simulation model that portrays the behavior of diverse operational, design, and other parameters. The flowchart for this stage is illustrated in Figure 3.3.

**Phase IV -A**

The initial phase of the CFD analysis involves the creation of a geometric model of the problem domain in accordance with the specifications. This geometric model can be generated using the design tool, specifically the Design Modeler integrated within ANSYS Workbench. Design Modeler offers a range of commands and tools for crafting both two-dimensional and three-dimensional representations of the relevant problem domain. In this context, the geometric model of the VIV turbine was crafted with the assistance of the Design Modeler within ANSYS Workbench. Moreover, a 3D model of the Bladeless turbine is created using the SolidWorks software as shown in figure 3.4. It consists of a mast made for solid rigid material (e.g., Carbon fiber, aluminum, Glass fiber, PVC etc.) and the flexible rod made of spring steel. The rod is made of elastic material as the mast oscillates under the force induced vortex. The simplicity of the structure and absence of moving parts like lot of bearings and gears reduces manufacturing, transport, and maintenance costs drastically. The dimensions of the bladeless turbine are as follows: The mast is of 130mm in height and 0.9mm in diameter. The flexible rod is 70mm in height. The whole system is placed in a rigid base.

**Phase IV -B**

Following the creation of the geometric model, the next step is the meshing process. During meshing, the problem domain is subdivided into a multitude of small cells, on which various equations are subsequently applied by the software.

**Phase IV -C**

Following the mesh generation, the next steps involve defining boundary conditions, various parameters, and equations. Initial conditions, final conditions, and governing equations play a pivotal role in computing the solution within the problem domain. The success of the research hinges on whether the obtained solution aligns with experimental results. If the simulation results are congruent with experimental findings, the research is deemed successful. However, if there is a disparity between the simulation and experimental outcomes, a reevaluation of the parameters is necessary, followed by a subsequent simulation iteration.
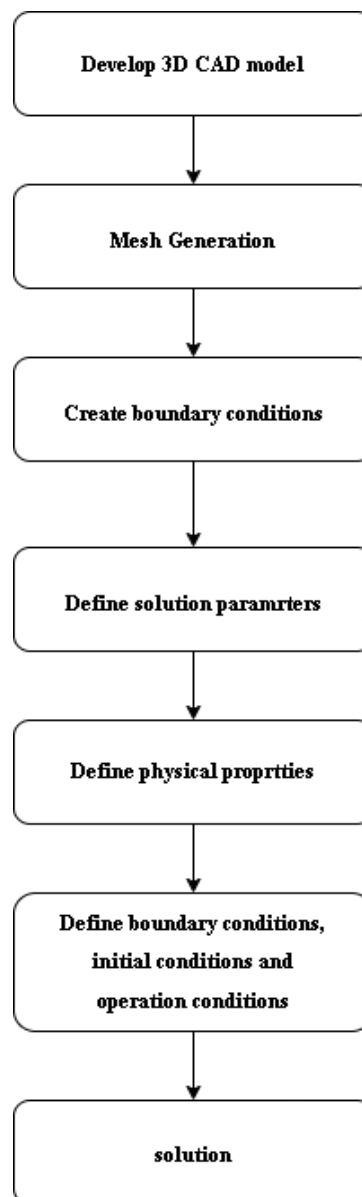


Figure 4.3: Flowchart of simulation and modeling

18

### 3.1.5    Phase V: Model verification and validation

The results derived from the CFD analysis solutions will be subjected to a thorough comparison with the experimental findings. Following this comparative analysis, a comprehensive conclusion will be drawn, accompanied by recommendations for potential avenues of improvement in future research endeavors.

### 3.1.6    Phase VI: Preparation of Thesis and Presentation

After obtaining the results, the research report will encompass all aspects of the study, ranging from idea inception to future prospects. Furthermore, a final presentation will be delivered on the scheduled date as per the directives of the relevant authority.

### 3.2 Numerical Method

### 3.2.1    SolidWorks 3-D CAD model

The 3D model of the Bladeless turbine is created using the SolidWorks software as shown in figure 3.4. It consists of a mast made for solid rigid material (e.g., Carbon fiber, aluminum, Glass fiber, PVC etc.) and the flexible rod made of spring steel.
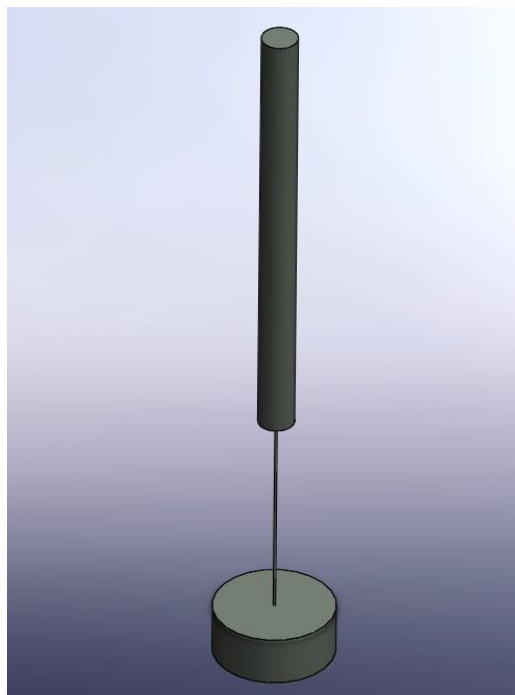


Figure 4.4: CAD model of VIV turbine

The rod is made of elastic material as the mast oscillates under the force induced by vortex. The simplicity of the structure and absence of moving parts like lot of bearings and gears reduces manufacturing, transport, and maintenance costs drastically (Ajay Kaviti & Amit Thakur, 2021). The dimensions of the bladeless turbine are as follows:

The mast is of 130mm in height and various diameter of 8mm, 10mm, 14mm in diameter. The flexible rod is 70mm in height. The whole system is placed on a rigid base.

### 3.2.2 Computational Fluid Dynamics (CFD)

To address the flow characteristics around a cylindrical bluff body comprehensively, a three-dimensional model is essential. This model needs to consider end effects and distinguish between parallel and oblique vortex shedding from the surface. Nevertheless, for a comprehensive assessment of how various system parameters (mass, stiffness, and damping) impact a cylinder's response to cross-flow, a two-dimensional (2-D) investigation was conducted and analyzed. The 2-D study facilitated the validation of numerical findings against experimental data while significantly reducing the overall computational expense compared to a 3-D numerical simulation. A comprehensive analysis of the problem at hand was made feasible through the application of Computational Fluid Dynamics (CFD).
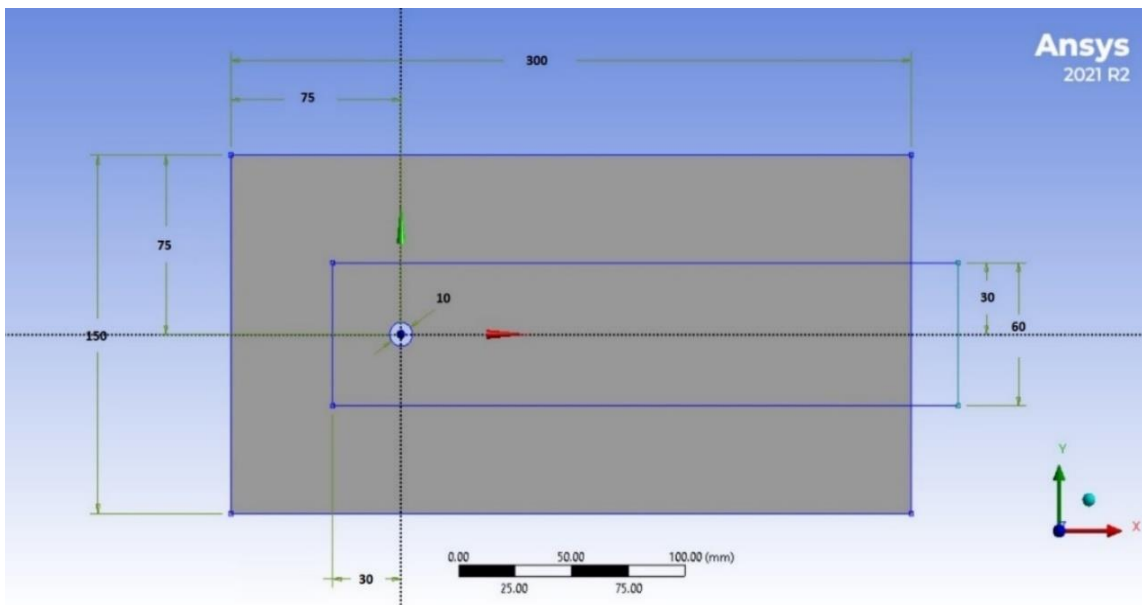


Figure 4.5: Geometry of computational domain (all dimensions are in mm)

CFD, a discipline within fluid mechanics, employs a range of numerical techniques and algorithms to solve governing equations, primarily involving the conservation of mass, momentum, and energy. These governing equations were integrated into the commercial CFD software, ANSYS FLUENT, which was utilized for solving the current problem.

### 3.2.3 Mesh Generation

The computational domain takes the form of a rectangular shape, measuring 300 millimeters in length and 150 millimeters in height. One of the longer sides of this

rectangle serves as the inlet, positioned closer to the cylinder, while the other serves as the outlet, located farther from the cylinder. The remaining two shorter sides are designated as walls. To obtain finer data around the cylindrical mast, an additional rectangle was created, measuring 60 millimeters in height and 255 millimeters in length. This geometry was constructed using the Design Modeler within the ANSYS software. Subsequently, the meshing process was performed, with a mesh size of 3 millimeters for the outer enclosure and 0.6 millimeters for the inner enclosure.

For improved resolution around the cylinder wall, the element face sizing was set to 3 millimeters and gradually increased up to 20 layers with a growth rate of 1.1, employing the inflation command. This meshing procedure resulted in a total of 54,713 nodes and 54,623 elements generated for the computation. The geometry and meshed model are depicted in figure 3.5 and 3.6.
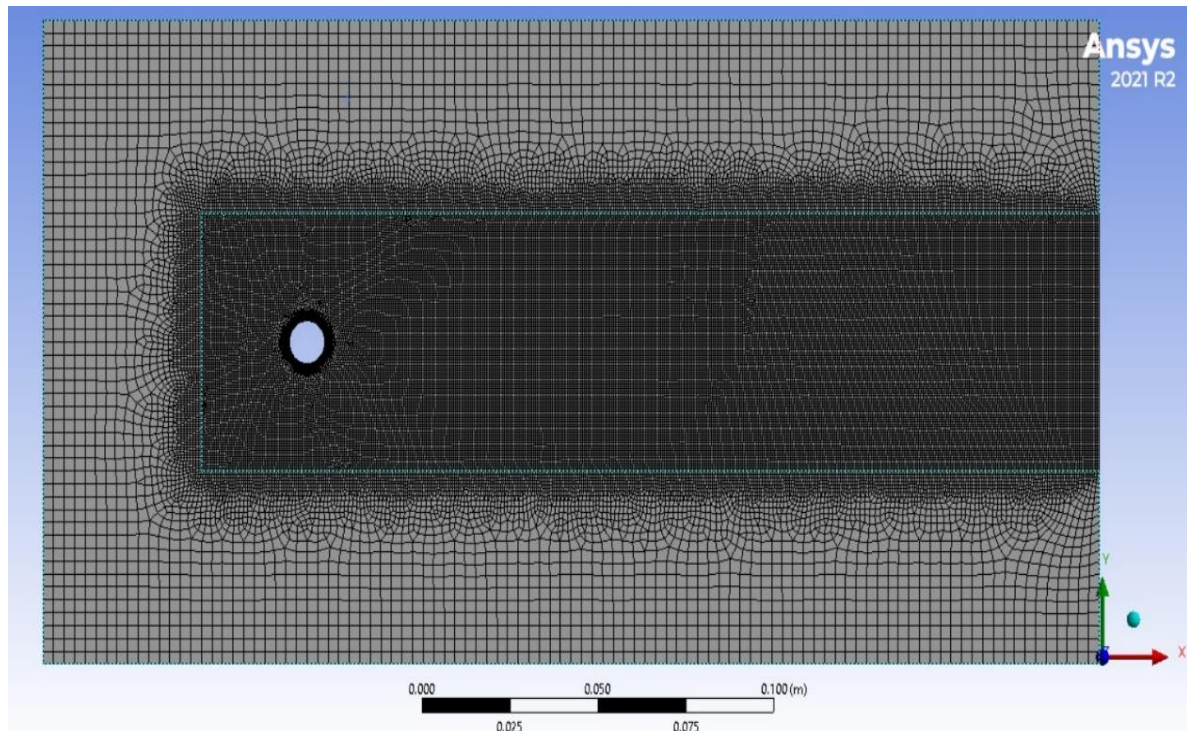


Figure 4.6:Meshed domain used in analysis

### 3.2.4 Boundary condition selection

The boundary conditions utilized in this numerical study are depicted in Figure 3.7 and comprise four distinct types:

- **Inlet**: The leftmost vertical boundary serves as the inlet, where the free stream velocity of the system is defined. The free stream velocity depends on the Reynolds number ($Re$), computed as $Re = ud/\nu$, where "$u$" represents the free stream velocity,

21

"*d*" is the diameter, and "*v*" signifies the kinematic viscosity of the fluid. Velocity is specified in its local Cartesian coordinate system as *U = (Ux, Uy, Uz)*, where *Ux* represents the velocity magnitude in the x-direction, while the y and z components of velocity are set to zero for this study.

- **Outlet**: Situated at the far downstream end of the domain, the outlet boundary condition prescribes the relative pressure over the entire boundary. In all simulations, the relative pressure at the outlet is specified as zero.

- **Symmetry**: Given that the entire simulation is a 2D model with infinite depth in the z-direction, symmetry boundary conditions are assigned to the front and back sides of the domain. This choice is made because ANSYS FLUENT cannot directly handle true 2D geometries.

- **Wall**: The wall boundary condition is commonly employed to separate the fluid region from the solid region. In this study, a "no-slip" wall boundary condition is applied to the cylinder's walls, meaning that the fluid's velocity at the wall surface is always set to zero (Uwall = 0).
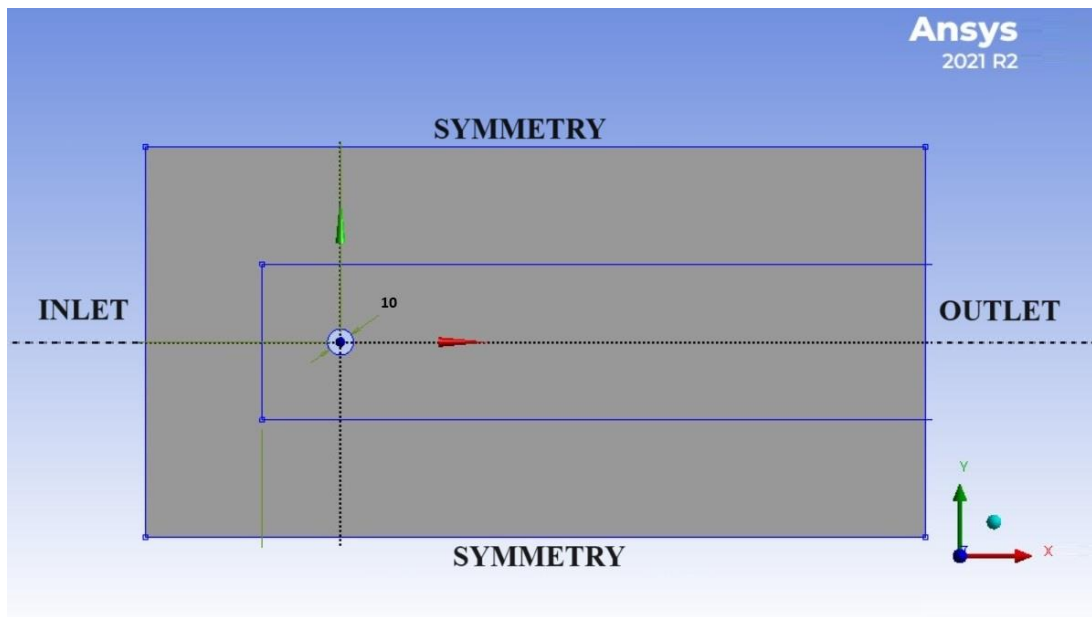


Figure 4.7: Boundary of computational domain

## 3.3 Experimental Steup

This section offers an overview of the experimental setup employed for the present Vortex-Induced Vibration (VIV) investigations. It includes details about the design of the experimental setup and the various diagnostic tools utilized.

The experiment was carried out in two separate ways one was done in laboratory while the other was done in a small stream near my village.

### 3.3.1 Laboratory setup

For the purpose of testing of model and data collection a laboratory setup was prepared. A water tank was made to hold the water and to mimic the flow of water a pump was used. The details of the setup is discussed below.

### 3.3.1.1 Test Tank

A glass tank of dimensions s 890mm×130mm×215mm ($l×b×h$) was made as shown in figure 3.8. A pump having discharge capacity ($Q_{max}$) of 1.5 m³/h was used. The water was pumped into the tank from the inlet side located on the right side of the tank and the water was pumped out of the tank from the outlet side located on the left side of the tank. A bunch of thin water straw of diameter 6mm was placed on the inlet side to make the water flow laminar.

As the pump was turned on a fluid flow velocity of 14 cm/s can be maintained in the setup tank. Because of budget constraint a large setup tank was not been able to be fabricated and the pump speed cannot be altered. Though a successful test of model was performed inside the tank, A successful model test was conducted within the tank, validating the proof of concept.
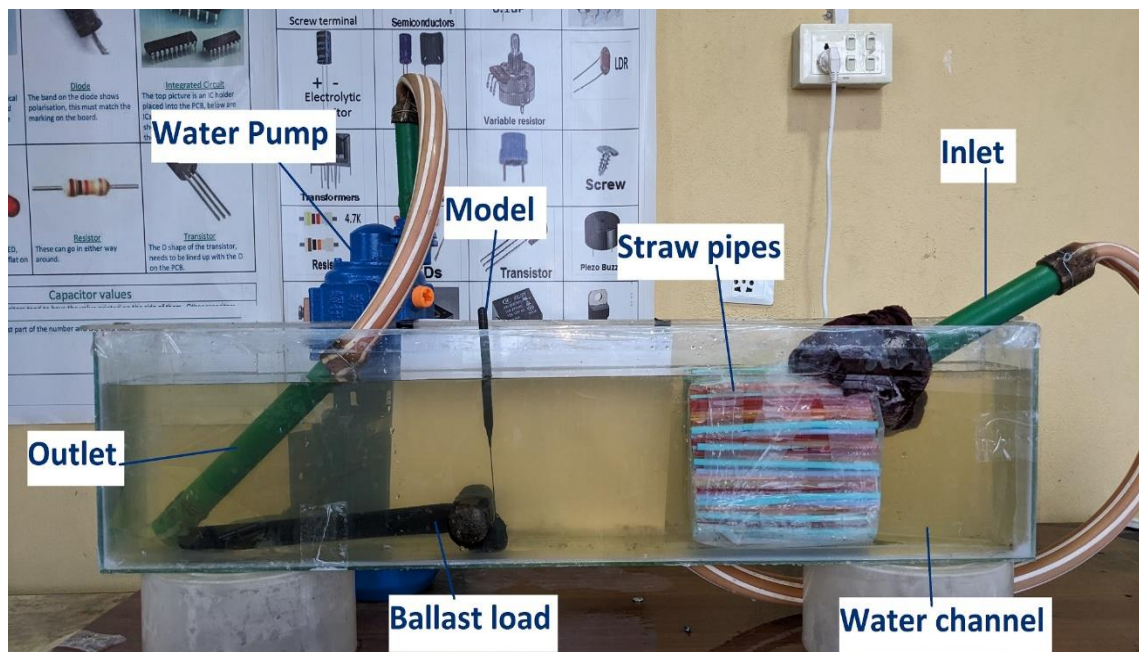


Figure 4.8: Setup tank for laboratory experiment

### 3.3.1.2 Prototype of VIV turbine

A cylindrical mast was used for the test purpose. The mast was made of a PVC tube of diameter 10mm and height of the mast was 130mm. A thin spring rod was attached with the mast which is made up of spring steel. It had a diameter of 0.8mm and length of 70mm. The whole system was anchored on a heavy ballast load so that it could firmly be placed on the bottom of the tank.

As the fluid flow past the cylindrical mast the vortex shedding induced an oscillatory force on the mast. The force and frequency of the displacement of the mast was crucial data for calculating the power generated from the turbine.



Figure 4.9: VIV turbine model attached to ballast tank

### 3.3.1.3 Details of water pump

The electrical water pump employed for the project has the following characteristics.

Table 4.1 Specifications of water pump

| Power | 1.1 kW |
|---|---|
| Head | 80m |
| Discharge | 1.5m$^3$/h |
| Rpm | 2850 |
| voltage | 220 V |
| Current | 6.5 A |
| Frequency | 50 Hz |

### 3.3.2   Tests conducted on natural Stream

A test on the natural stream was conducted Bhot Khola stream located on Gorkha district, Nepal. A channel was made by placing boulders and stoned forming a deep channel of depth 40 cm and width 43 cm. A decent amount of flow was obtained in the stream. The flow velocity was calculated using float method and found to be 19.8 cm/s on the surface.

Three different cylindrical mast having different dimensions were tested on the stream.



Figure 4.10: Testing model on Bhot khola stream, Gorkha

The results of all of the turbines were noted and used for the analysis on the following chapter.

For the test purpose the turbine of the following dimensions was used.:

**Dimension of Model 1**: Diameter: 8mm, Length of mast: 100mm, length of spring rod: 80mm, total length of system: 180mm

**Dimension of Model 2**: Diameter: 10mm, length of mast: 100mm, Length of spring rod: 80mm, total length of the system: 180mm.

**Dimension Model 3**: Diameter: 14mm, length of mast: 100mm, Length of spring rod: 80mm, total length of the system: 180mm.

The density of fluid is taken to be **998kg/m$^3$**.



Figure 4.12: Different dimensions of turbines model
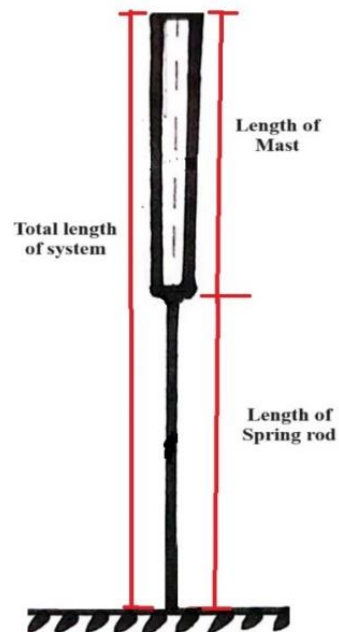


Figure 4.11: Dimension of VIV turbine

### 3.3.3 Determination of flow velocity
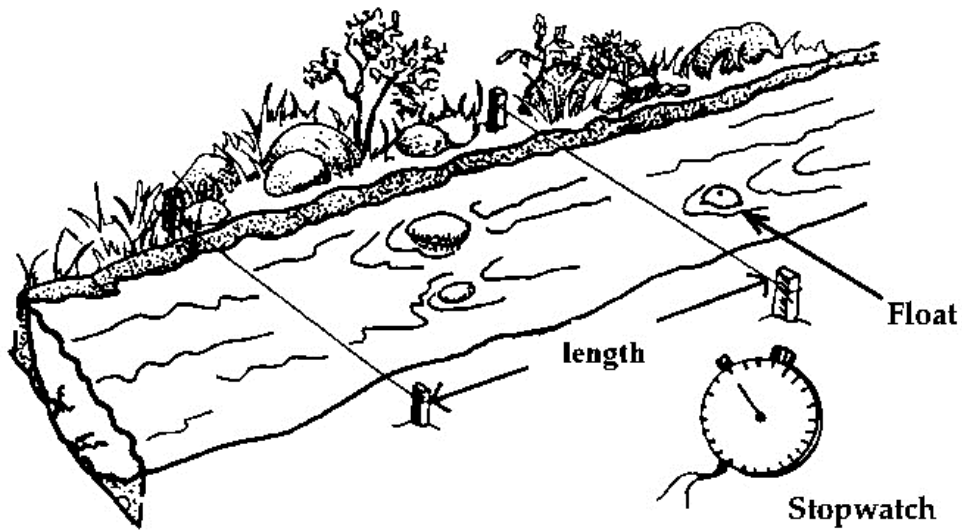


Figure 4.13: Float method of flow velocity measurement

Float method is a most popular method for measurement of stream velocity. This method quantifies surface velocity and calculates the mean velocity using a correction factor. The fundamental concept involves measuring the time it takes for an object to travel a defined distance downstream while floating. This method is majorly used in calculation of discharge of water in micro hydro power.

The flow velocity is calculate using following equation:

$$surface\ flow\ velocity(V_{mean}) = \frac{distance\ travelled}{time} \qquad (2)$$

Surface velocities are typically greater than mean or average velocities. The relationship between them is expressed as,

$$V_{mean} = kV_{surface} \qquad (3)$$

where "$k$" is a coefficient that typically falls within the range of 0.66 to 0.75, depending on the channel's depth.

Table 4.2: Correction factor

| Coefficients for Converting Float Velocity to Mean Channel | |
|---|---|
| **Average Depth (ft)** | **Coefficient** |
| 1 | 0.66 |
| 2 | 0.68 |
| 3 | 0.7 |
| 4 | 0.72 |
| 5 | 0.74 |
| 12 | 0.78 |
| *Source: USBR, 1997* | |

For the river stream following data were tabulated and flow velocity was calculated in the next topic.
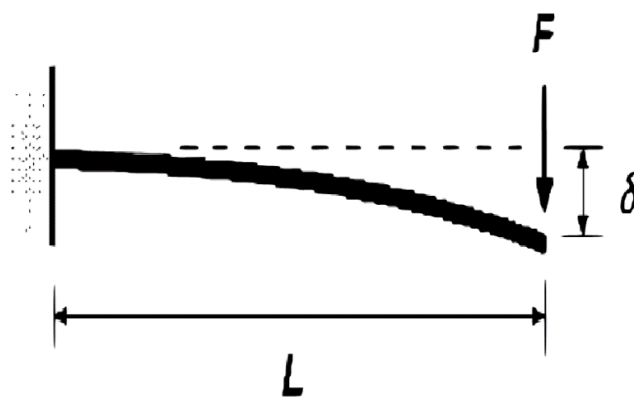


Figure 4.14: Deflection of cantilever soring rod under action of force

### 3.3.4   Energy stored in the cantilever spring rod

One end of the spring is anchored, while the opposite end is allowed to move freely, giving it the characteristics of a cantilever spring, illustrated in Figure 3.14. The symbol

"$\delta$" represents the deflection of the slender rod. "$F$" denotes the force applied to the free end of the rod, and "$L$" stands for the length of the rod. The equation governing the potential energy stored in the wire is expressed by Equation (4), as the rod undergoes deformation due to an external force.

$$Strain\ Energy = \frac{1}{2} \times Force\ \times Deflection \tag{4}$$

We know,

$$deflection(\delta) = \frac{FL^3}{3EI} \tag{5}$$

Where,

    $F$ = Force applied on the free end of rod

    $L$ = Length of the rod

    $E$ = Modulus of elasticity

    $I$ = Moment of inertia

    From equations (2) and (3), we get

$$Strain\ energy\ (U) = \frac{F^2L^3}{6EI} \tag{6}$$

### 3.3.5 Power extracted by the turbine

To calculate the power extracted by the turbine the time period should be determined.

Then the time taken by the turbine to move from mean position to the maximum displaced position is determined. Then we know,

$$Power\ extracted\ (P) = \frac{Energy\ extracted(E)}{time\ taken\ to\ deflect\ maximum\ deflected\ position\ to\ mean\ position(t)} \tag{7}$$

# CHAPTER FOUR: RESULTS AND DISCUSSION

## 4.1 Results obtained from experiments

The flow velocity of the stream was calculated to be **19.8 cm/s** by taking the value of **k** to be **0.66.**

Using similar method, the flow velocity of the setup tank was measured to be **14cm/s** and the mean velocity to be 0.66×14 = **9.24 cm/s.**

Table 5.1: Flow velocity calculations

| S.N. | Length of channel(cm) | Time taken (s) | Surface velocity of stream (cm/s) | Average surface velocity (cm/sec) | Mean flow velocity(cm/sec) |
|------|------|------|------|------|------|
| 1 | 130 | 3.68 | 35.33 | | |
| 2 | 130 | 4.26 | 30.52 | | |
| 3 | 130 | 4.39 | 29.61 | | |
| 4 | 130 | 4.87 | 26.69 | | |
| 5 | 130 | 5.29 | 24.57 | | |
| 6 | 130 | 5.11 | 25.44 | | |
| 7 | 130 | 4.27 | 30.44 | 30 | 19.8 |
| 8 | 130 | 4.5 | 28.89 | | |
| 9 | 130 | 3.81 | 34.12 | | |
| 10 | 130 | 3.9 | 33.33 | | |
| 11 | 130 | 3.9 | 33.33 | | |
| 12 | 130 | 4.6 | 28.26 | | |
| 13 | 130 | 4.41 | 29.48 | | |

## 4.1.1 Measurement of mast displacement

The displacement of the mast was measured using scale and vernier calipers. The following data was measured in which different flow velocity and diameter of mast was used. The displacement was taken for a spring length of 800mm.

Table 5.2: Peak-peak displacement of turbine

| S.N. | Flow velocity (cm/s) | Diameter of cylinder(mm) | Submerged Height (mm) | Peak-peak displacement (mm) |
|------|------|------|------|------|
| 1 | 9.24 | 8 | 100 | 24 |
| 2 | 9.24 | 10 | 100 | 29 |
| 3 | 9.24 | 14 | 100 | 28 |
| 4 | 19.8 | 8 | 100 | 26 |
| 5 | 19.8 | 10 | 100 | 32 |
| 6 | 19.8 | 14 | 100 | 34 |

### 4.1.2 Determination of modulus of elasticity

The modulus of elasticity "$E$" for the rod was determined through another series of experiments. In this experiment, a known weight was suspended from the free end of the rod, and the resulting deflection "$\delta$" was measured. The rod has a diameter of 0.8 mm. A weight of 74 grams was hung at a distance of 100 mm from the free end, resulting in a deflection of the rod measuring 15.7 mm.
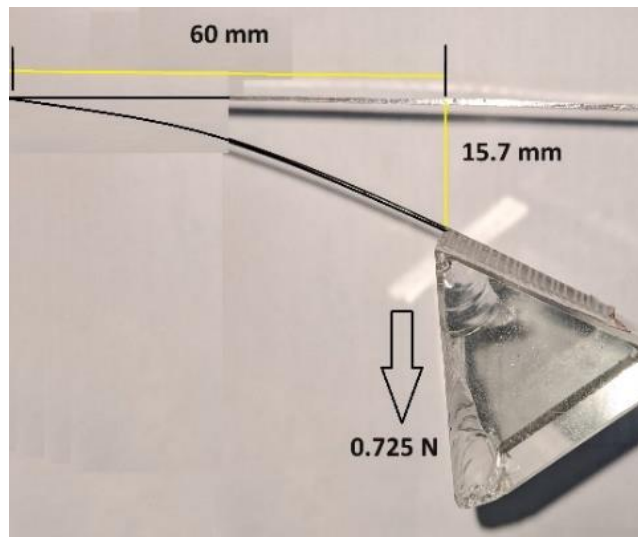


Figure 5.1: Deflection of cantilever spring

For a rod with a circular cross-section, the moment of inertia "$I$" is calculated as follows:

$$I = \frac{\pi d^4}{64} \tag{8}$$

$$= 0.02 \text{mm}^2$$

Using Equation (2), the value of the modulus of elasticity "E" is determined to be **166,242.03 N/mm²**.

### 4.1.3 Determination of deflection of rod

The rod is deflected by the hydrodynamic forces around the mast. The maximum peak to peak displacement is measured to be 29 mm at the top point of the mast. But we need to measure the displacement of spring under water, for this a approximation approach is taken since for very small deflection the rod acts as a straight rod but for larger deflection parabolic equation needs to be considered. As total peak to peak deflection of top point of mast is 29 mm, i.e., in figure 4.2, AB = 14.5 mm. Total length of mast and rod, OA = 180 mm. Hence,

Angle of deflection ($\theta$) = $\sin^{-1}$(AB/OA) = 14.5/0 = 4.62°

The length of the spring rod is 80 mm. Then, the

deflection CD ($\delta$) = 80 ∗ sin4.62° = 6.44 mm.
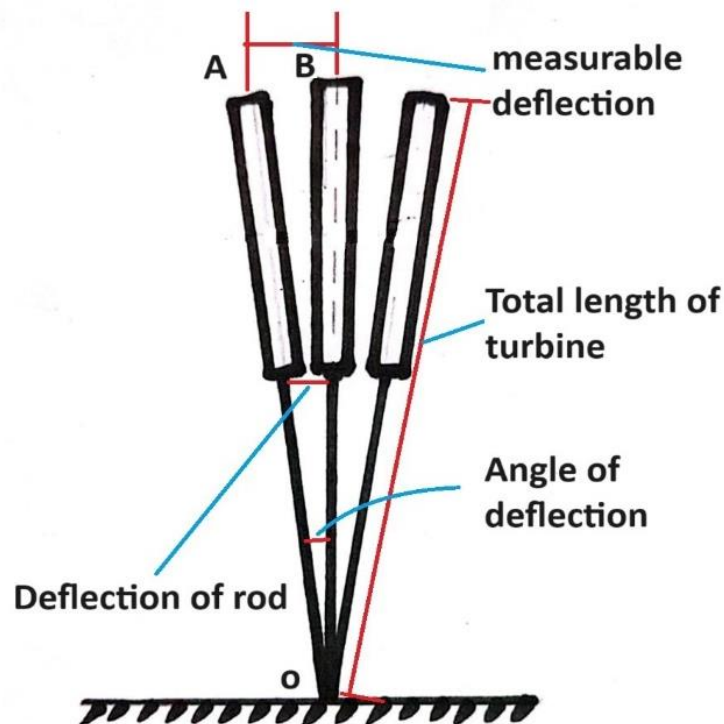


Figure 5.2: Representation of the turbine

Table 5.4: Deflection of rod only for flow velocity 19.8cm/s

| Flow velocity = 19.8cm/s | | | | | | |
|---|---|---|---|---|---|---|
| Diameter of cylinder (mm) | Peak-peak displacement (mm) | Length of rod (mm) | Length of mast and rod(mm) | Peak displacement AB (mm) | Angle of deflection (θ) (radian) | Deflection of rod only (mm) |
| 8 | 26 | 80 | 180 | 13 | 0.0723 | 5.78 |
| 10 | 32 | 80 | 180 | 16 | 0.089 | 7.11 |
| 14 | 34 | 80 | 180 | 17 | 0.0946 | 7.56 |

Table 5.3: Deflection of rod for flow velocity 9.24cm/s

| Flow velocity = 9.24 cm/s | | | | | | |
|---|---|---|---|---|---|---|
| Diameter of cylinder (mm) | Peak-peak displacement (mm) | Length of rod (mm) | Length of mast and rod(mm) | Peak displacement AB (mm) | Angle of deflection (θ) (radian) | Deflection of rod only (mm) |
| 8 | 24 | 80 | 180 | 12 | 0.0667 | 5.33 |
| 10 | 29 | 80 | 180 | 14.5 | 0.0806 | 6.44 |
| 14 | 28 | 80 | 180 | 14 | 0.0779 | 6.23 |

### 4.1.4   Determination of energy stored in the spring rod

From equation (2) the force exerted on the free end of flexible cantilever rod is given by,

$$F = \frac{3EI\delta}{L^3} \tag{9}$$

$$= \frac{3 \times 166242.03 \times 0.02 \times 5.33}{80^3}$$

$$= 0.1039$$

The force experienced on the free end of the wire **F = 0.10384 N.** The calculated force on other data is shown on table below.

Table 5.6:Force exerted of the free end of spring for flow velocity 19.8 cm./s

| flow velocity = 19.8cm/s | | | | | | | |
|---|---|---|---|---|---|---|---|
| diameter of cylinder (mm) | Peak-peak displacement (mm) | length of rod (mm) | length of mast and rod(mm) | peak displacement AB (mm) | Angle of deflection ($\theta$) (radian) | Deflection of rod only (mm) | Force (N) |
| 8 | 26 | 80 | 180 | 13 | 0.07228516 | 5.7777778 | 0.11256 |
| 10 | 32 | 80 | 180 | 16 | 0.08900636 | 7.1111111 | 0.13854 |
| 14 | 34 | 80 | 180 | 17 | 0.09458541 | 7.5555556 | 0.14719 |

Table 5.5: Force exerted of the free end of spring for flow velocity 9.24 cm./s

| Flow velocity = 9.24 cm/s | | | | | | | |
|---|---|---|---|---|---|---|---|
| diameter of cylinder (mm) | Peak-peak displacement (mm) | length of rod (mm) | length of mast and rod(mm) | peak displacement AB (mm) | Angle of deflection ($\theta$) (radian) | Deflection of rod only (mm) | Force (N) |
| 8 | 24 | 80 | 180 | 12 | 0.06671615 | 5.3333333 | 0.1039 |
| 10 | 29 | 80 | 180 | 14.5 | 0.08064293 | 6.4444444 | 0.12555 |
| 14 | 28 | 80 | 180 | 14 | 0.07785641 | 6.2222222 | 0.12122 |

As the energy stored in the wire is provided by the fluid forces, it is equal to the energy extracted by the bladeless turbine.

$$E = \frac{1}{2} \times Force \ \times Deflection \qquad (10)$$

$$= \frac{1}{2} \times 0.1039 \ \times \frac{5.33}{1000}$$

$$= 0.000277 \ J$$

Hence, the energy extracted by VIV turbine of diameter 8mm for a flow velocity of 9.24cm/s is **0.000277J**.

Table 5.7: Energy stored in spring for flow velocity 9.24cm/s & 19.8cm/s

| Flow velocity = 9.24 cm/s | | |
|---|---|---|
| Deflection of rod only (mm) | Force (N) | Energy stored in wire(J) |
| 5.33 | 0.1038363 | 0.000276724 |
| 6.44 | 0.1254608 | 0.000403984 |
| 6.23 | 0.1213697 | 0.000378067 |
| Flow velocity = 19.8cm/s | | |
| Deflection of rod only (mm) | Force (N) | Energy stored in wire(J) |
| 5.78 | 0.112603 | 0.000325423 |
| 7.11 | 0.1385134 | 0.000492415 |
| 7.56 | 0.14728 | 0.000556719 |

## 4.1.5 Determination of oscillation frequency of turbine

The oscillation frequency was determined by counting the oscillations and measuring time with a stopwatch. The data shows different frequencies of oscillation which are dependent on the velocity of flow and the diameter of turbine. For a lower flow velocity, the frequency of oscillation in less for same diameter of the turbine. The following table shows the comparison of different diameter of turbine with different flow velocities. Table 4.9 shows oscillation or resonant frequency of turbine at flow velocity 9.24 cm/s and table 4.10 shows resonant frequency of turbine at flow velocity 19.8 cm/s. The following data was taken from the observation.

Table 5.8: Oscillation frequency for flow velocity 9.24cm/s

| Actual data Flow velocity = 9.24cm/s | | |
|---|---|---|
| Diameter of cylinder (mm) | Average time taken for one oscillation(s) | Frequency of oscillation (Hz) |
| 8 | 0.38 | 2.63 |
| 10 | 0.4 | 2.5 |
| 14 | 0.8 | 1.25 |

Table 5.9: Oscillation frequency for flow velocity 19.8cm/s

| Actual data Flow velocity = 19.8cm/s | | |
|---|---|---|
| Diameter of cylinder (mm) | Average time taken for one oscillation(s) | Frequency of oscillation (Hz) |
| 8 | 0.29 | 3.45 |
| 10 | 0.38 | 2.63 |
| 14 | 0.48 | 2.08 |

## 4.1.6 Determination of power extracted by turbine

The power that is produced by the turbine can be determined as follows:

$$Power(P) = \frac{Energy\ extracted(E)}{Time(T)} \qquad (11)$$

Table 5.10: Power extracted by turbine for different flow velocity

| Actual data Flow velocity = 9.24cm/s | | | | |
|---|---|---|---|---|
| Diameter of cylinder (mm) | Average time taken for one oscillation(s) | Time taken to reach from mean position to peak position(s) | Energy extracted (J) | power calculated (W) |
| 8 | 0.38 | 0.095 | 0.00027707 | 0.0029165 |
| 10 | 0.4 | 0.1 | 0.000404542 | 0.0040454 |
| 14 | 0.8 | 0.2 | 0.000377123 | 0.0018856 |
| Actual data Flow velocity = 19.8cm/s | | | | |
| Diameter of cylinder (mm) | Average time taken for one oscillation(s) | Time taken to reach from mean position to peak position(s) | Energy extracted (J) | power calculated (W) |
| 8 | 0.29 | 0.0725 | 0.000325172 | 0.0044851 |
| 10 | 0.38 | 0.095 | 0.000492569 | 0.0051849 |
| 14 | 0.48 | 0.12 | 0.000556064 | 0.0046339 |

## 4.2 Results obtained from CFD simulation

The simulation of various diameter of turbines was carried out on different flow velocities. The results are shown below.

### 4.2.1 Turbine diameter 8mm flow velocity 9.24cm/s

From figure 4.3, for a bluff cylinder of diameter 8mm and flow velocity of 9.24cm/s vertex shedding phenomenon is present. The free stream velocity is 9.24 cm/s and it is seen that there is a velocity increment up to 14.55cm/s since there is flow around the curvature of the bluff body. It is seen from the figure 4.3 that there is a periodic shedding of vortex around the bluff body. This periodic change in velocity induces lift forces and drag force as well. These periodic forces the body to swing periodically and it reaches the resonance frequency of the turbine.

In simulation the oscillation frequency was obtained to be **2.87 Hz**.

From equation (1), i.e.,

$$S = \frac{f_s D}{U}$$

$$or, f_s = \frac{S U}{D}$$

Putting the value of $S = 0.2$, $U = 9.24$cm/s, $D = 8$mm, we get, $f_s = 2.31$ **Hz**. This shows similarities of simulation results with theoretical research.



Figure 5.3: Vortex shedding in turbine of diameter 8mm at flow velocity 9.24cm/s

Figure 5.4: (a) Velocity contour in x- axis only, (b) velocity counter in y- axis only, (c) velocity contour in z- axis only, (d) pressure distribution around the mast

The velocity contour of the turbine of 8mm diameter in the flow velocity of 9.24 cm/s has been divided into respective three-dimensional axes. This shows that the fluid has a changing velocity in two spatial dimensions u and v out of three spatial dimensions (*u, v, w*). Figure 4.4 (a) shows the change in fluid velocity in *u* direction. The velocity of the fluid is increased up to 14.36 cm/s in the forward direction and reduced up to 3cm/s in the reversed direction. Figure 4.4 (b) shows the fluid velocity in *v* direction. The velocity of fluid changes is increased up to 10cm/s in the forward direction and reduced up to 9.27cm/s in reversed direction. Figure 4.4 (c) shows that there is no change in *w* direction. Figure 4.4(d) is visual representation of pressure distribution around the turbine. The maximum pressure of 5.16 Pascals can be seen in the front face of the turbine.

38

Figure 5.5: (a) coefficient of lift, (b) coefficient of drag, (c) coefficient of momentum, (d) force plot for turbine of 8 mm diameter and 9.24cm/s velocity

The simulation result of turbine of diameter 8 mm diameter shows that there is oscillatory motion of the turbine at a low flow velocity of 9.24cm/s. This shows that there is a periodic hydrodynamic force acting on the turbine which can be harnessed by a suitable power take off mechanism. The periodic motion is seen on the figure 4.5 (c) where the plot of momentum is depicted. The time period of one complete oscillation was measured from the graphical method and the average time period of one complete oscillation is measured to be 0.348 second measured from the graph. Hence, the oscillation frequency or the resonance frequency of the turbine is found to be 2.87 Hz. Figure 4.5 (a) Shows that there is a periodic change in coefficient of lift from positive to negative values. This means that the force is changing directions in a periodic manner which is the base for Vortex Induced Vibrations. The flow of fluid is directly facing the turbine so there is a drag force associated with it. But compared to lift force drag force is constant and it shows miniscule oscillation motion. The drag coefficient was found to be averaging on 1.5 as shown in figure 4.5 (b). The force of drag is around 0.05 newton on the turbine shown in figure 4.5(d).

## 4.2.2 Turbine diameter 10mm flow velocity 9.24cm/s

From figure 4.6, for a bluff cylinder of diameter 8mm and flow velocity of 9.24 cm/s vertex shedding phenomenon is present. The free stream velocity is 9.24 cm/s and it is seen that there is a velocity increment up to 15.79 cm/s since there is flow around the curvature of the bluff body. It is seen from the figure 4.6 that there is a periodic shedding of vortex around the bluff body. This periodic change in velocity induces lift forces and drag force as well. These periodic forces the body to swing periodically and it reaches the resonance frequency of the turbine.

In simulation, the oscillation frequency was obtained to be **2.3 Hz**.

From equation (1),

Putting the value of

Strouhal Number $(S)$ = 0.2,

Freestream velocity of fluid $(U)$ = 9.24cm/s,

Diameter of cylinder $(D)$ = 10mm,

The Frequency of oscillation of the cylinder , $\boldsymbol{f_s = 1.85\ Hz}$.

This shows some deviation of simulation results with theoretical research.
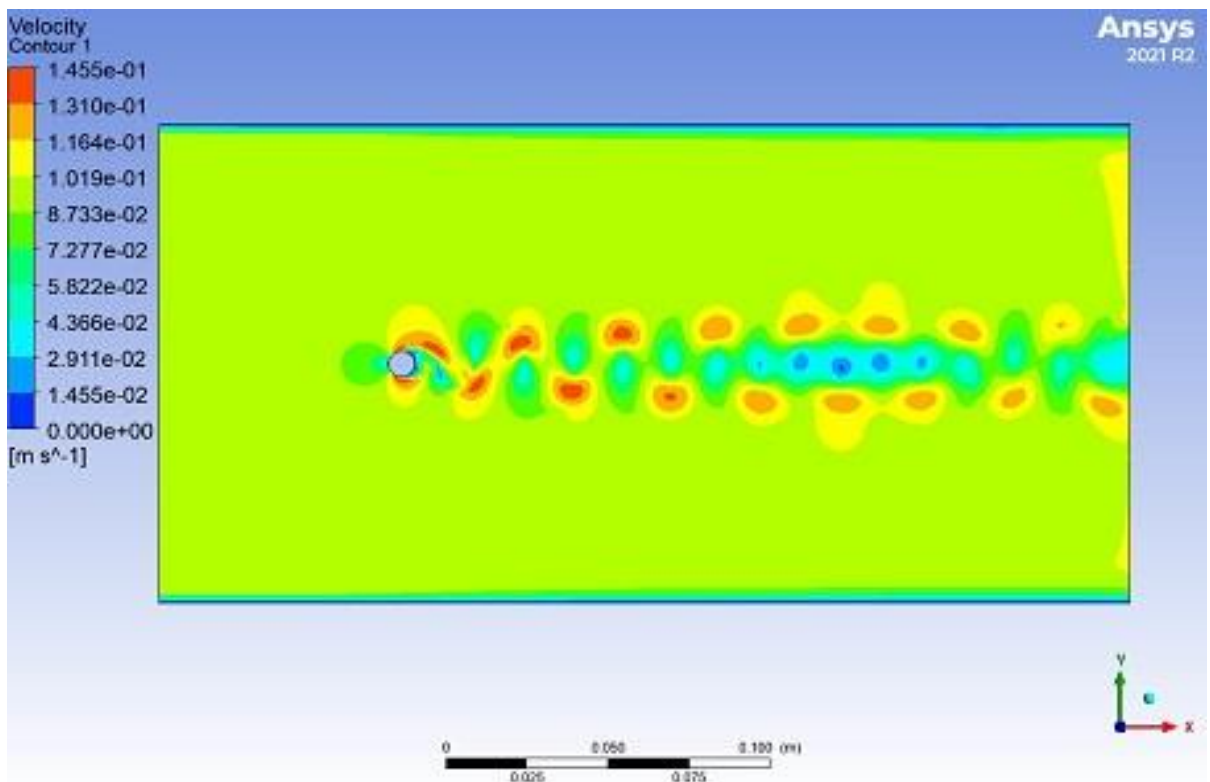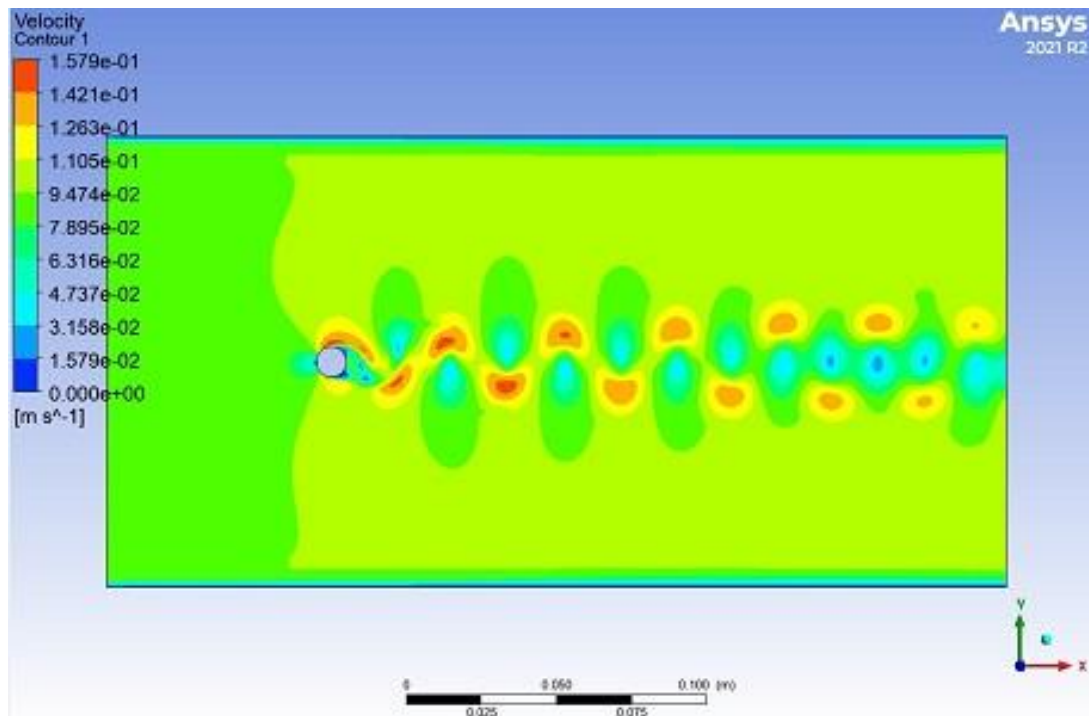


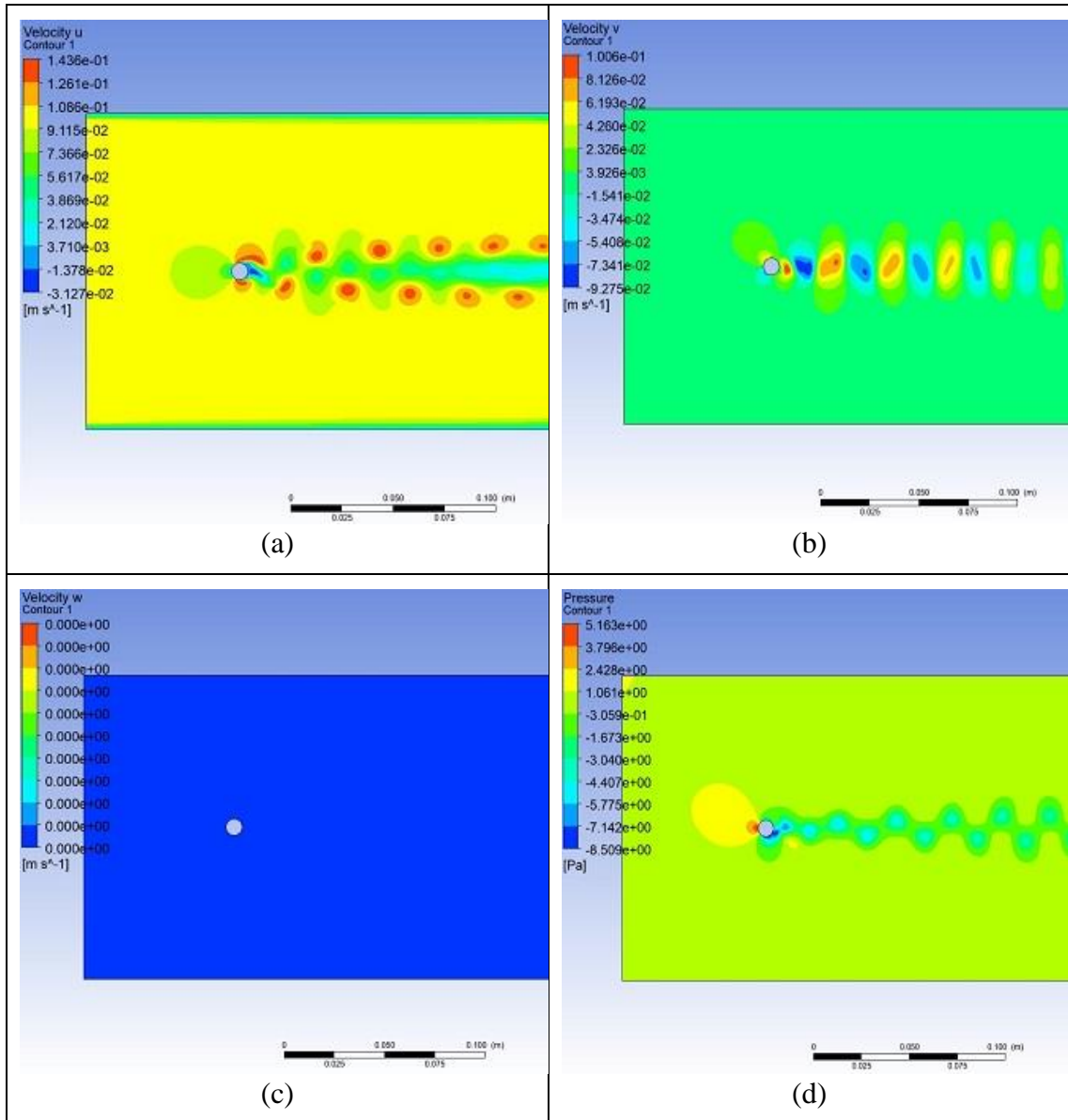Figure 5.6: Vortex shedding in turbine of diameter 10mm at flow velocity 9.24cm/s

Figure 5.7: (a) Velocity contour in x- axis only, (b) velocity counter in y- axis only, (c) velocity contour in z- axis only, (d) pressure distribution around the mast

The velocity contour of the turbine of 10 mm diameter in the flow velocity of 9.24 cm/s has been divided into respective three-dimensional axes. This shows that the fluid has a changing velocity in two spatial dimensions u and v out of three spatial dimensions (*u, v, w*). Figure 4.7 (a) shows the change in fluid velocity in *u* direction. The velocity of the fluid is increased up to 15.49 cm/s in the forward direction and reduced up to 5.8 cm/s in the reversed direction. Figure 4.7 (b) shows the fluid velocity in *v* direction. The velocity of fluid changes is increased up to 9.45 cm/s in the forward direction. Figure 4.7 (c) shows that there is no change in *w* direction.  Figure 4.7(d) is visual representation of pressure

41

distribution around the turbine. The maximum pressure of 5.16 Pascals can be seen in the front face of the turbine.
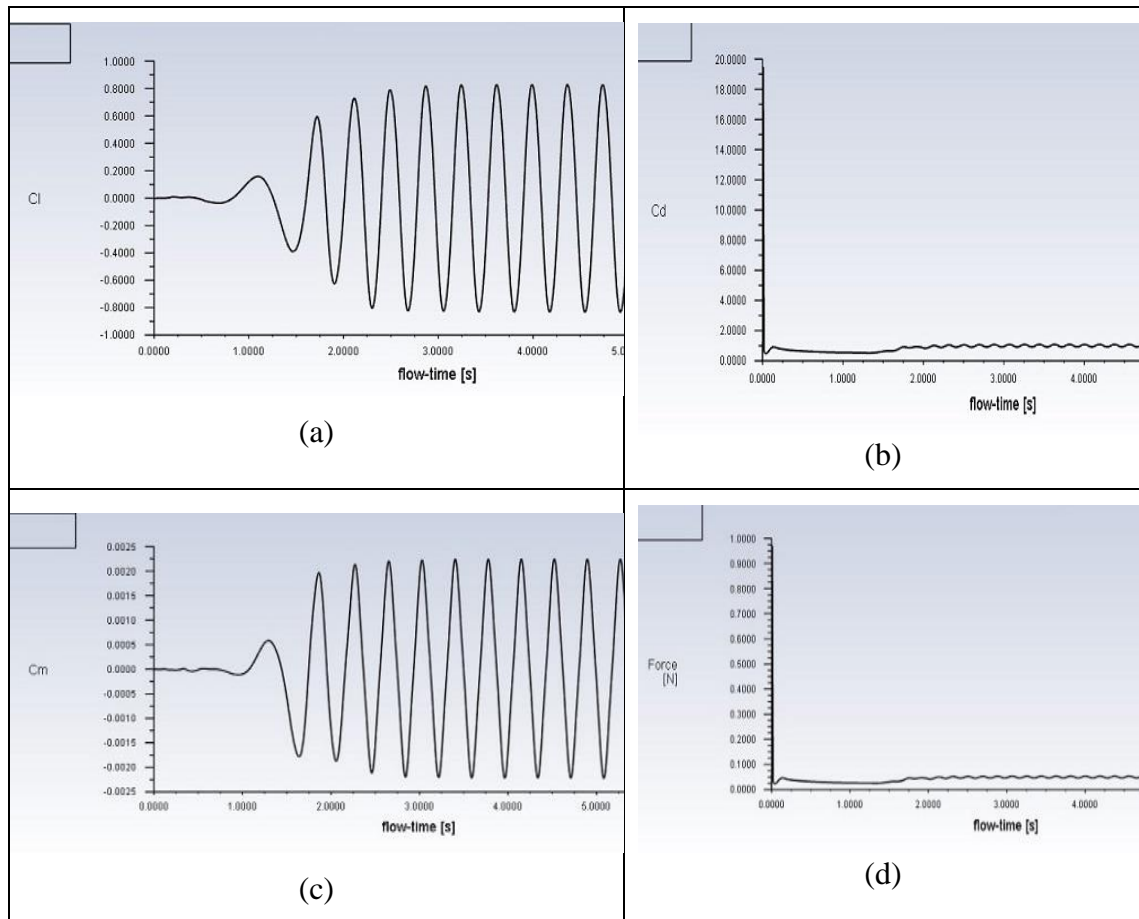


Figure 5.8: (a) coefficient of lift, (b) coefficient of drag, (c) coefficient of momentum, (d) force plot for turbine of 10mm diameter and 9.24cm/s velocity

The simulation result of turbine of diameter 10mm diameter shows that there is oscillatory motion of the turbine at a low flow velocity of 9.24cm/s. This shows that there is a periodic hydrodynamic force acting on the turbine which can be harnessed by a suitable power take off mechanism. The periodic motion is seen on the figure 4.8 (c) where the plot of momentum is depicted. The time period of one complete oscillation was measured from the graphical method and the average time period of one complete oscillation is measured to be 0.435 second measured from the graph. Hence, the oscillation frequency or the resonance frequency of the turbine is found to be 2.3 Hz.Figure 4.8 (a) Shows that there is a periodic change in coefficient of lift from positive to negative values. This means that the force is changing directions in a periodic manner which is the base for Vortex Induced Vibrations. The flow of fluid is directly facing the turbine so there is a

42

drag force associated with it. But compared to lift force drag force is constant and it shows miniscule oscillation motion. The drag coefficient was found to be averaging on 2.5 as shown in figure 4.8 (b). The force of drag is around 0.1 newton on the turbine shown in figure 4.8 (d).

### 4.2.3 Turbine diameter 14mm flow velocity 9.24cm/s

From figure 4.9, for a bluff cylinder of diameter 8mm and flow velocity of 9.24cm/s vertex shedding phenomenon is present. The free stream velocity is 9.24 cm/s and it is seen that there is a velocity increment up to 17.22 cm/s since there is flow around the curvature of the bluff body. It is seen from the figure 4.9 that there is a periodic shedding of vortex around the bluff body. This periodic change in velocity induces lift forces and drag force as well. These periodic forces the body to swing periodically and it reaches the resonance frequency of the turbine.

In simulation, the oscillation frequency was obtained to be **1.8 Hz**.

From equation (1),

Putting the value of

> Strouhal Number (*S)* = 0.2,
> Freestream velocity of fluid (*U*) = 9.24cm/s,
> Diameter of cylinder (*D*) = 14mm,

The Frequency of oscillation of the cylinder , $f_s = \mathbf{1.32}$ **Hz**.

This shows few deviations of simulation results with theoretical research.
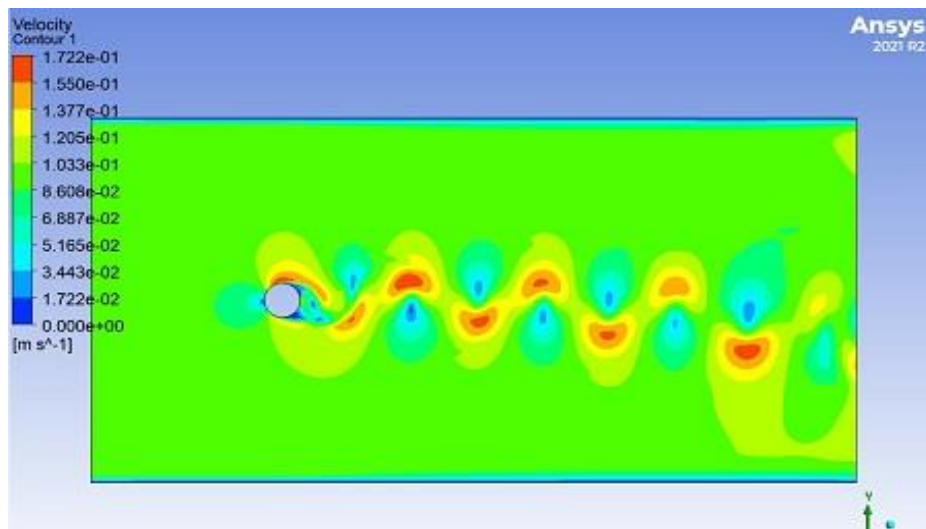


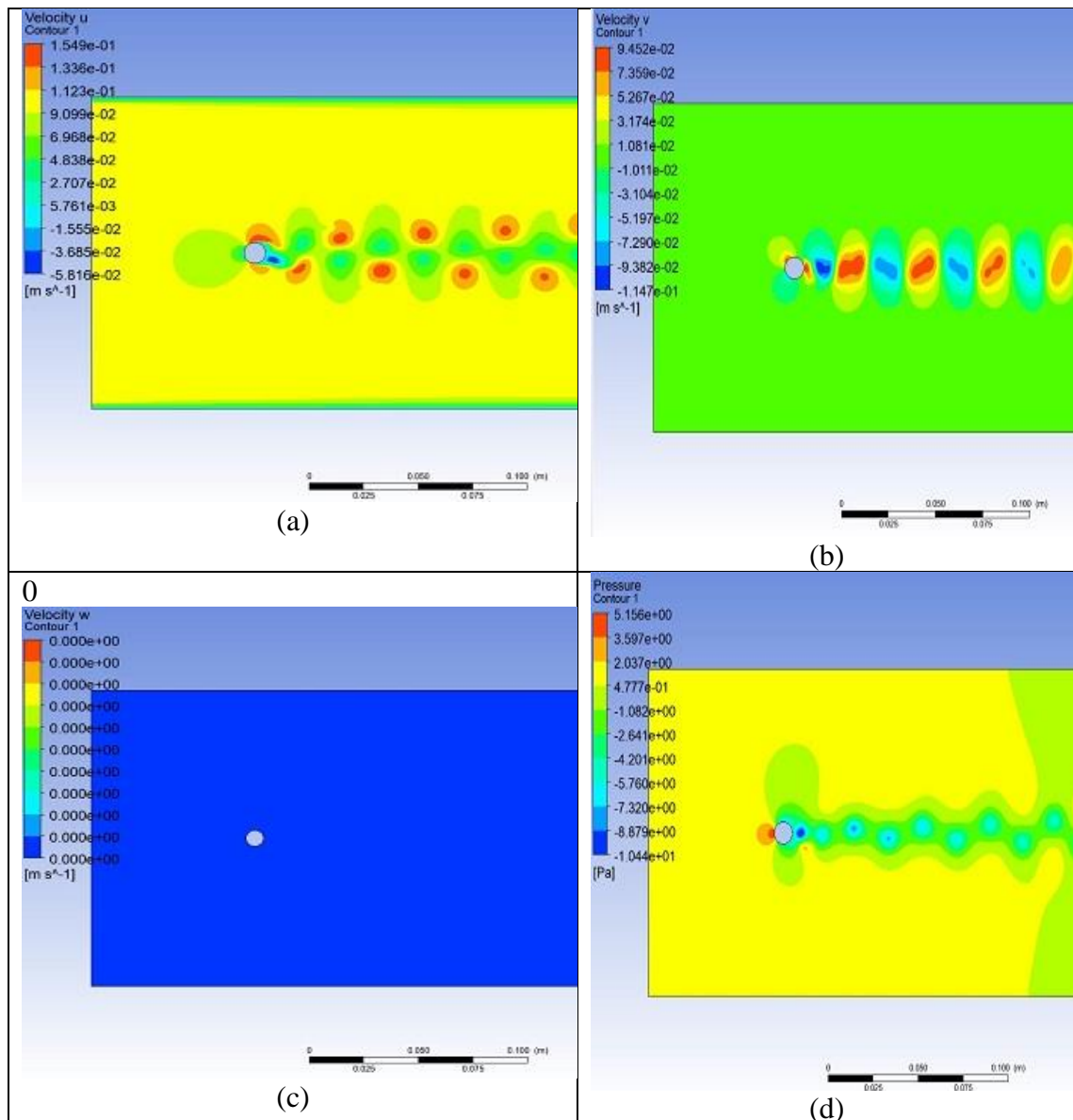Figure 5.9: Vortex shedding in turbine of diameter 14mm at flow velocity 9.24cm/s

Figure 5.10: (a) Velocity contour in x- axis only, (b) velocity counter in y- axis only,
(c) velocity contour in z- axis only, (d) pressure distribution around the mast

The velocity contour of the turbine of 14 mm diameter in the flow velocity of 9.24 cm/s has been divided into respective three-dimensional axes. This shows that the fluid has a changing velocity in two spatial dimensions u and v out of three spatial dimensions (*u, v, w*). Figure 4.10 (a) shows the change in fluid velocity in *u* direction. The velocity of the fluid is increased up to 17.12 cm/s in the forward direction and reduced up to 6 cm/s in the reversed direction. Figure 4.10 (b) shows the fluid velocity in *v* direction. The velocity of fluid changes is increased up to 10 cm/s in the forward direction and reduced upto 12.9 cm/s in reversed direction. Figure 4.10 (c) shows that there is no change in *w* direction. Figure 4.10(d) is visual representation of pressure distribution around the turbine. The maximum pressure of 5.56 Pascals can be seen in the front face of the turbine.
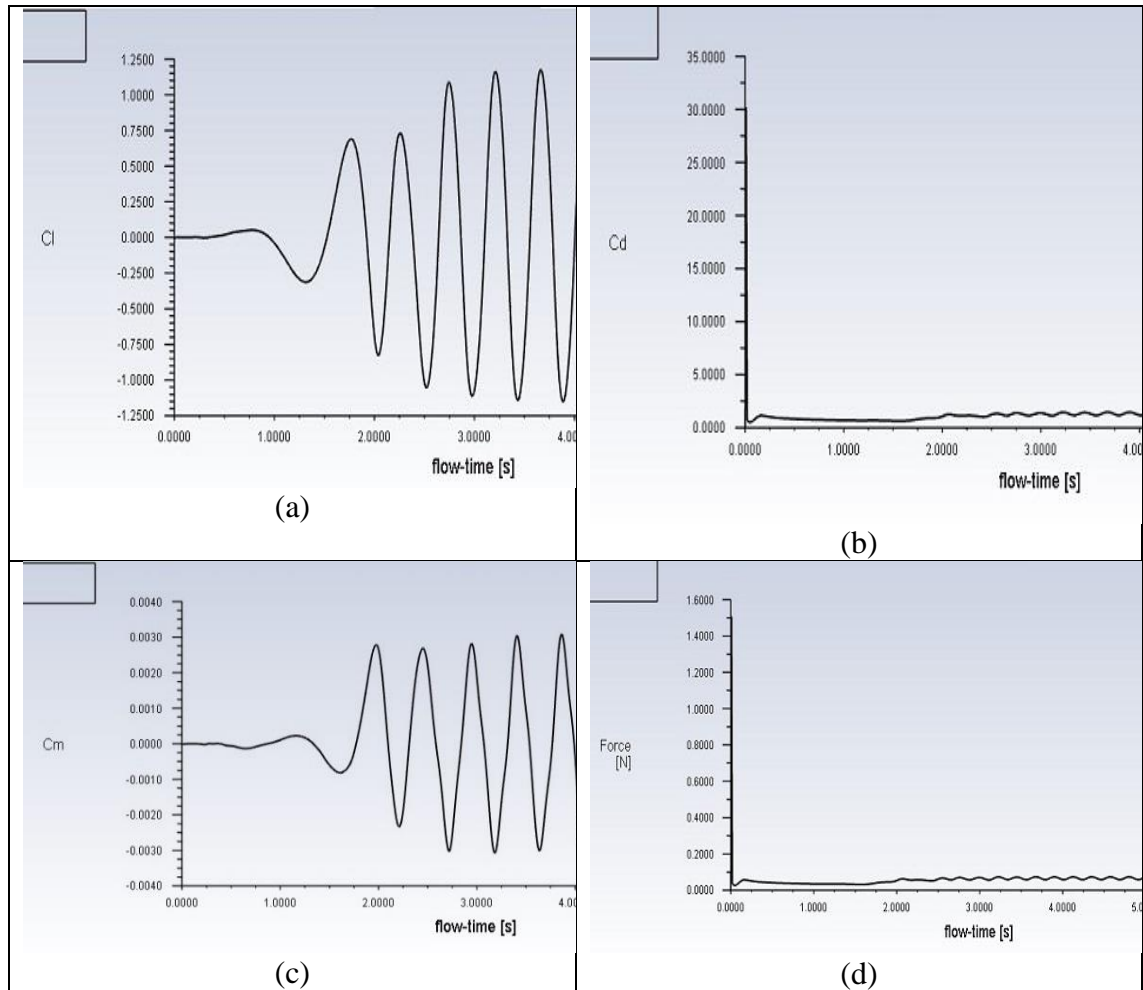
44

Figure 5.11: (a) coefficient of lift, (b) coefficient of drag, (c) coefficient of momentum, (d) force plot for turbine of 14mm diameter and 9.24cm/s velocity

The simulation result of turbine of diameter 14mm diameter shows that there is oscillatory motion of the turbine at a low flow velocity of 9.24cm/s. This shows that there is a periodic hydrodynamic force acting on the turbine which can be harnessed by a suitable power take off mechanism. The periodic motion is seen on the figure 4.11 (c) where the plot of momentum is depicted. The time period of one complete oscillation was measured from the graphical method and the average time period of one complete oscillation is measured to be 0.555 second measured from the graph. Hence, the oscillation frequency or the resonance frequency of the turbine is found to be 1.8 Hz. Figure 4.11 (a) Shows that there is a periodic change in coefficient of lift from positive to negative values. This means that the force is changing directions in a periodic manner which is the base for Vortex Induced Vibrations. The flow of fluid is directly facing the turbine so there is a

45

drag force associated with it. But compared to lift force drag force is constant and it shows miniscule oscillation motion. The drag coefficient was found to be averaging on 2.5 as shown in figure 4.11 (b). The force of drag is around 0.1 newton on the turbine shown in figure 4.11(d).

### 4.2.4    Turbine diameter 8 mm flow velocity 19.8 cm/s

From figure 4.12, for a bluff cylinder of diameter 8mm and flow velocity of 19.8cm/s vertex shedding phenomenon is present. The free stream velocity is 19.8 cm/s and it is seen that there is a velocity increment up to 36.55 cm/s since there is flow around the curvature of the bluff body. It is seen from the figure 4.12 that there is a periodic shedding of vortex around the bluff body. This periodic change in velocity induces lift forces and drag force as well. These periodic forces the body to swing periodically and it reaches the resonance frequency of the turbine.

In the simulation the oscillation frequency was obtained to be **3.4 Hz**.

From equation (1),

> Putting the value of
> Strouhal Number ($S$) = 0.2,
> Freestream velocity of fluid ($U$) = 19.8 cm/s,
> Diameter of cylinder ($D$) = 8 mm,

The Frequency of oscillation of the cylinder , $f_s = 4.95$ Hz.

This shows some deviation of simulation results with theoretical research.
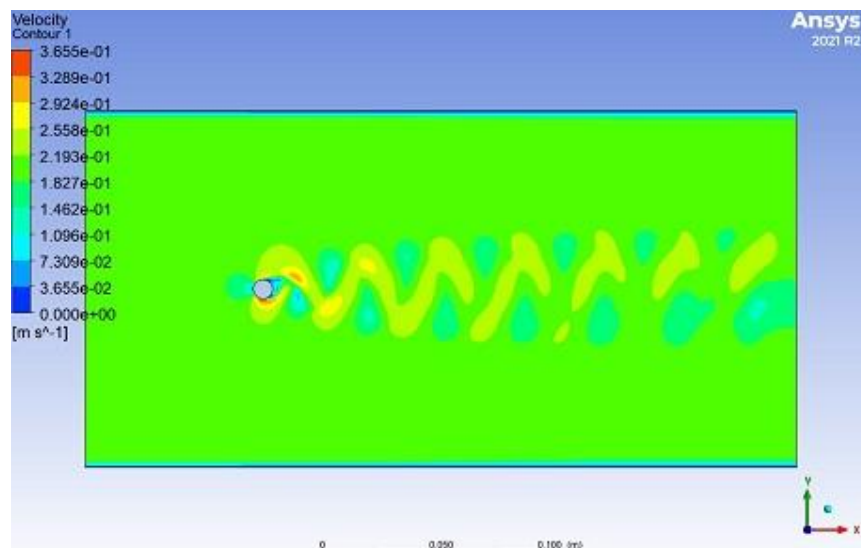


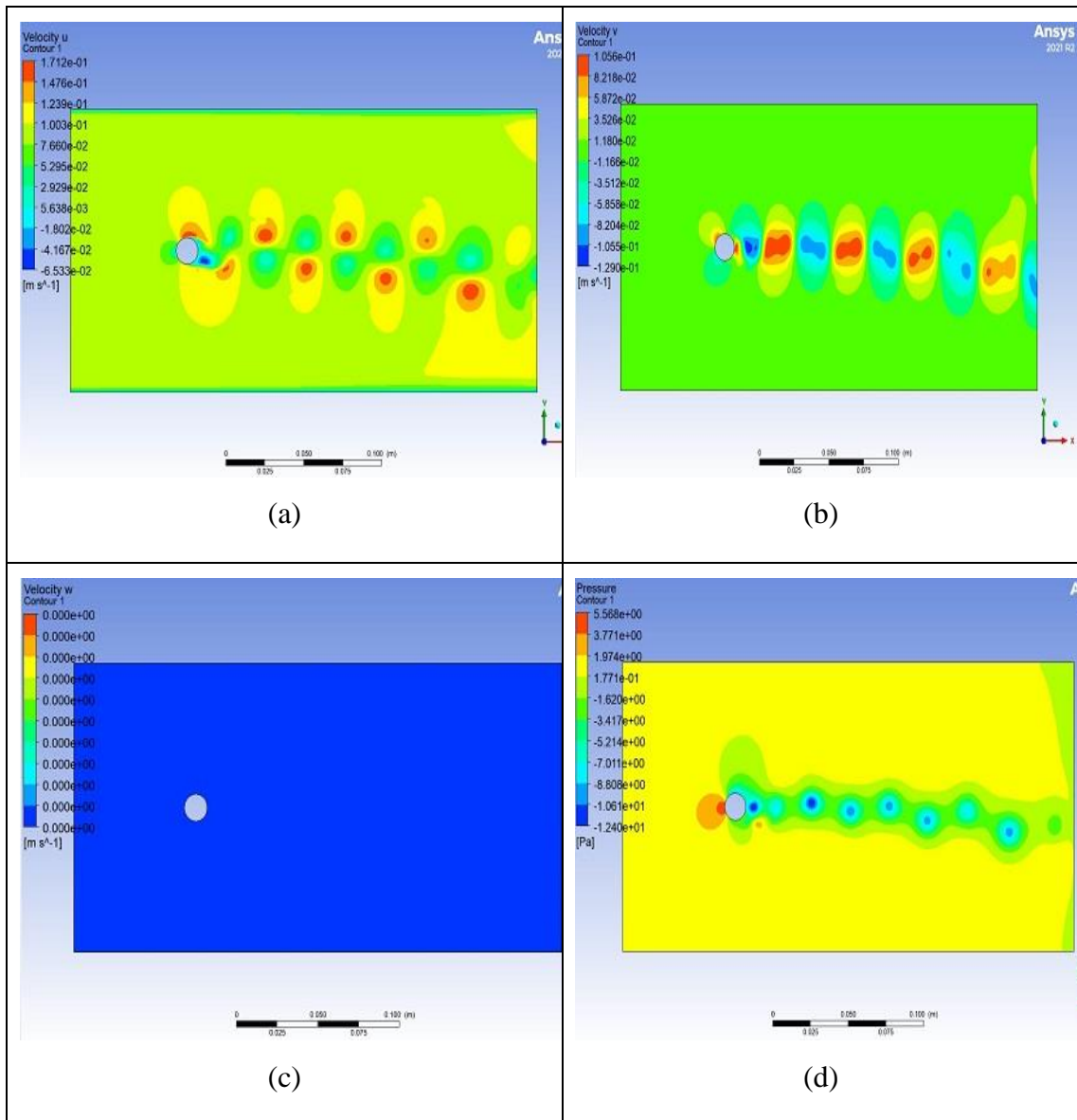Figure 5.12: Vortex shedding in turbine of diameter 8mm at flow velocity 19.8 cm/s

Figure 5.13: (a) Velocity contour in x- axis only, (b) velocity counter in y- axis only, (c) velocity contour in z- axis only, (d) pressure distribution around the mast

The velocity contour of the turbine of 8 mm diameter in the flow velocity of 19.8 cm/s has been divided into respective three-dimensional axes. This shows that the fluid has a changing velocity in two spatial dimensions u and v out of three spatial dimensions (*u, v, w*). Figure 4.13 (a) shows the change in fluid velocity in *u* direction. The velocity of the fluid is increased up to 36.44 cm/s in the forward direction and reduced up to 21.52 cm/s in the reversed direction. Figure 4.13 (b) shows the fluid velocity in *v* direction. The velocity of fluid changes is increased up to 24.7 cm/s in the forward direction and reduced up to 22.15 cm/s in reversed direction. Figure 4.13 (c) shows that there is no change in *w*

47

direction. Figure 4.13 (d) is visual representation of pressure distribution around the turbine. The maximum pressure of 21.7 Pascals can be seen in the front face of the turbine.
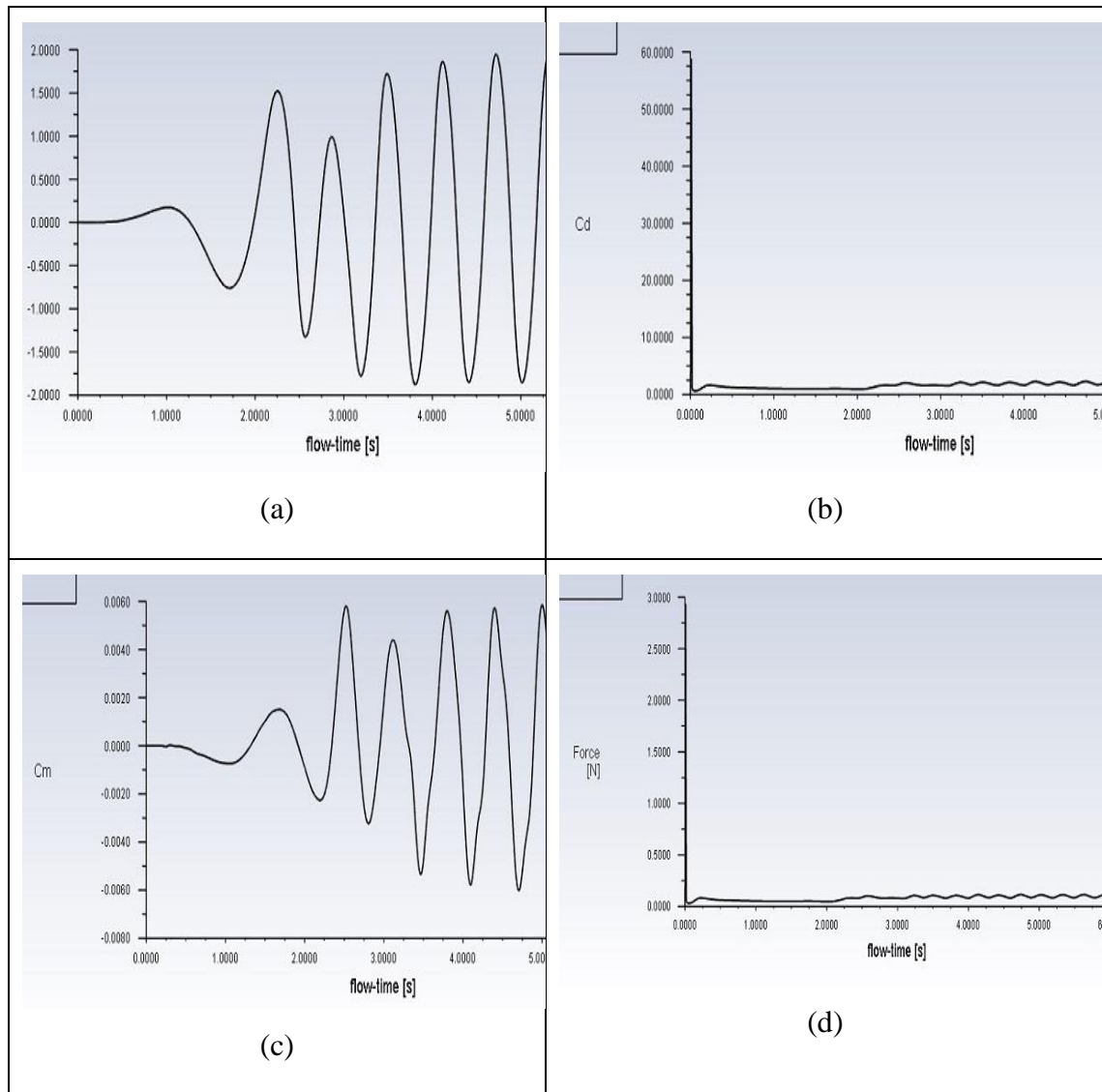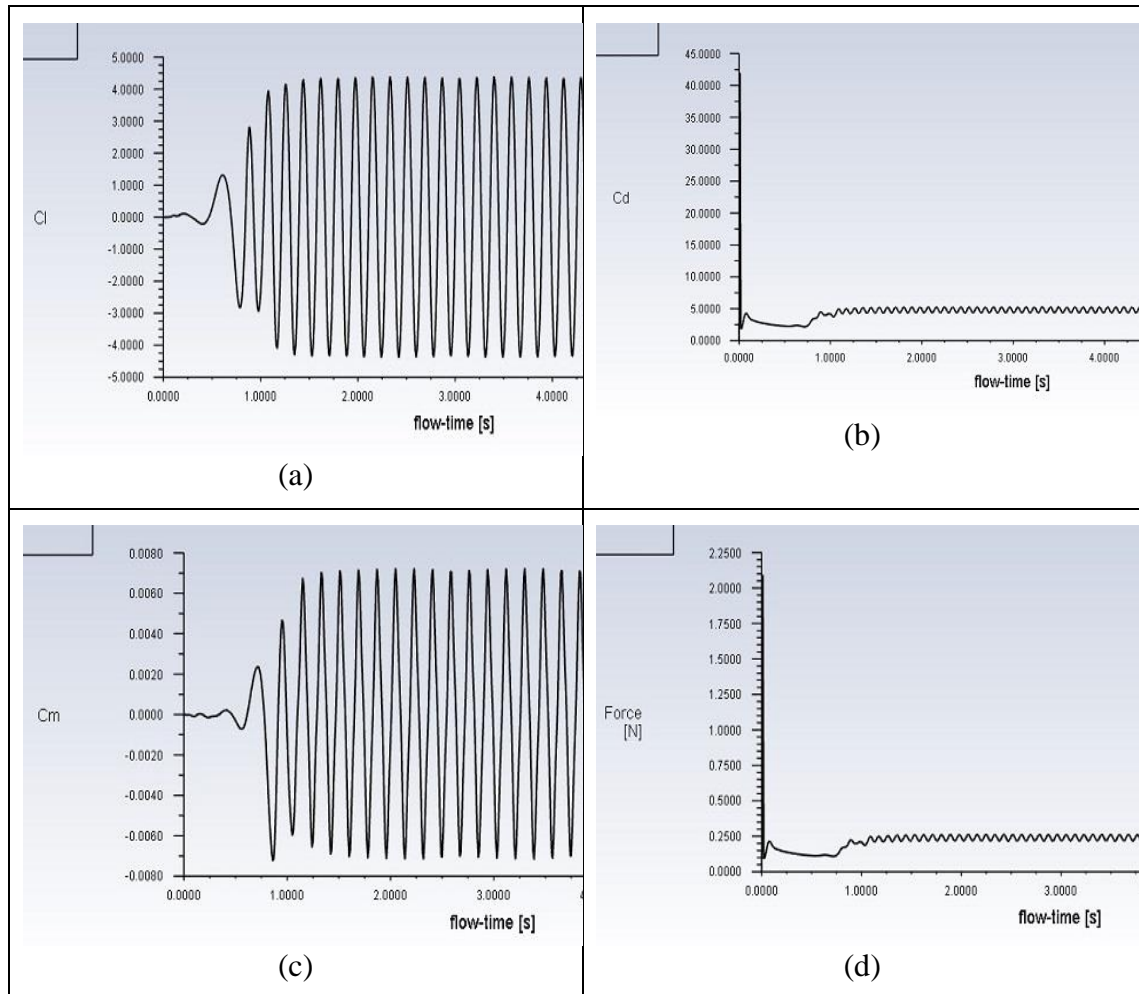


Figure 5.14: (a) coefficient of lift, (b) coefficient of drag, (c) coefficient of momentum, (d) force plot for turbine of 8mm diameter and 19.8cm/s velocity

The simulation result of turbine of diameter 8mm diameter shows that there is oscillatory motion of the turbine at a low flow velocity of 19.8 cm/s. This shows that there is a periodic hydrodynamic force acting on the turbine which can be harnessed by a suitable power take off mechanism. The periodic motion is seen on the figure 4.14 (c) where the plot of momentum is depicted. The time period of one complete oscillation was measured from the graphical method and the average time period of one complete oscillation is measured to be 0.294 second measured from the graph. Hence, the oscillation frequency or the resonance frequency of the turbine is found to be 3.4 Hz.Figure 4.14 (a) Shows that there is a periodic change in coefficient of lift from positive to negative values. This means that the force is changing directions in a periodic manner which is the base for Vortex Induced Vibrations. The flow of fluid is directly facing the turbine so there is a

drag force associated with it. But compared to lift force drag force is constant and it shows miniscule oscillation motion. The drag coefficient was found to be averaging on 5 as shown in figure 4.14 (b). The force of drag is around 0.25 newton on the turbine shown in figure 4.14 (d).

### 4.2.5   Turbine diameter 10mm flow velocity 19.8cm/s

From figure 4.15, for a bluff cylinder of diameter 8mm and flow velocity of 19.8 cm/s vertex shedding phenomenon is present. The free stream velocity is 19.8 cm/s and it is seen that there is a velocity increment up to 32.36 cm/s since there is flow around the curvature of the bluff body. It is seen from the figure 4.15 that there is a periodic shedding of vortex around the bluff body. This periodic change in velocity induces lift forces and drag force as well. These periodic forces the body to swing periodically and it reaches the resonance frequency of the turbine.

In the simulation the oscillation frequency was obtained to be **3.23 Hz**.

From equation (1),

Putting the value of

   Strouhal Number (*S)* = 0.2,
   Freestream velocity of fluid (*U*) = 19.8 cm/s,
   Diameter of cylinder (*D*) = 10 mm,

The Frequency of oscillation of the cylinder , $f_s = 3.96\ Hz$.

This shows few deviations of simulation results with theoretical research.
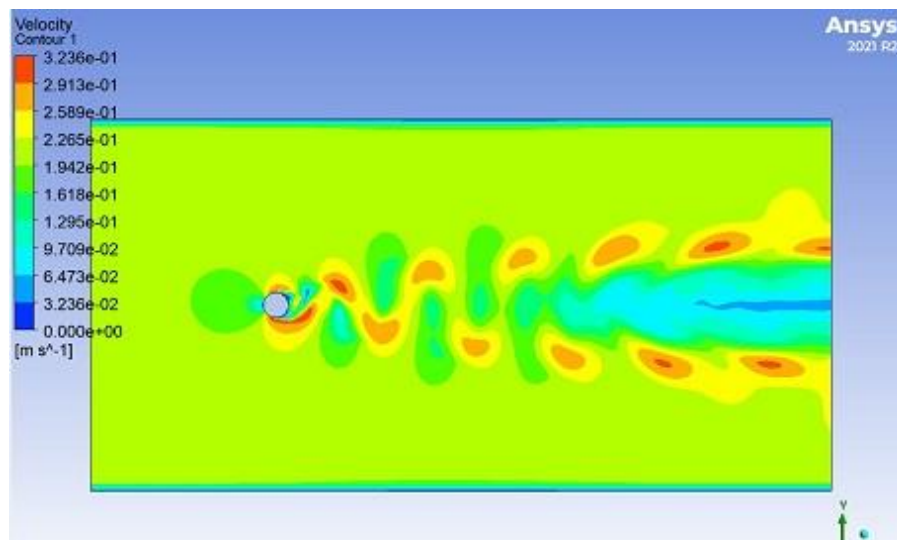


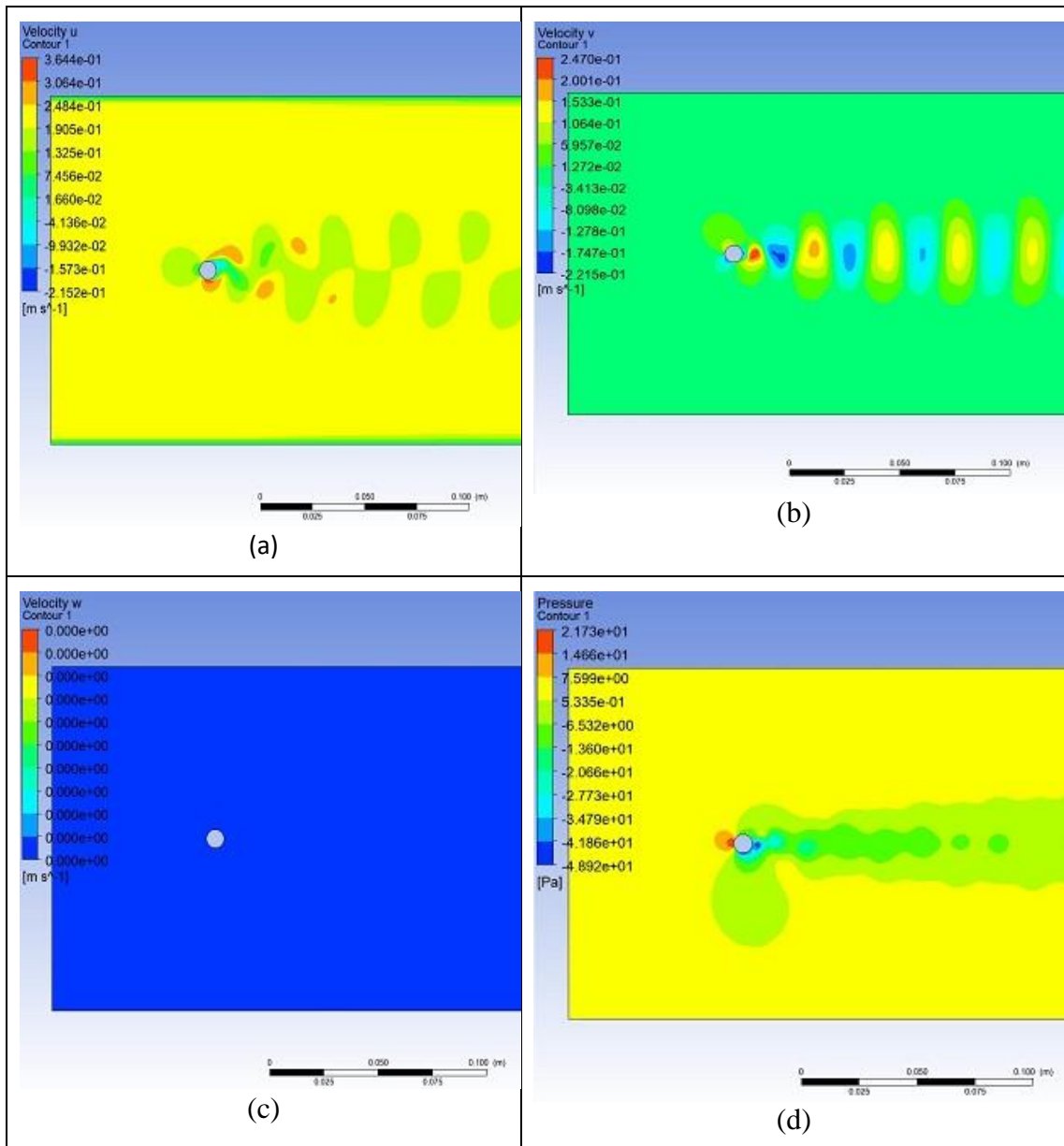Figure 5.15: Vortex shedding in turbine of diameter 10mm at flow velocity 19.8cm/s

Figure 5.16: (a) Velocity contour in x- axis only, (b) velocity counter in y- axis only, (c) velocity contour in z- axis only, (d) pressure distribution around the mast

The velocity contour of the turbine of 10 mm diameter in the flow velocity of 19.8 cm/s has been divided into respective three-dimensional axes. This shows that the fluid has a changing velocity in two spatial dimensions u and v out of three spatial dimensions ($u$, $v$, $w$). Figure 4.16 (a) shows the change in fluid velocity in $u$ direction. The velocity of the fluid is increased up to 31.03 cm/s in the forward direction and reduced up to 10.64 cm/s in the reversed direction. Figure 4.16(b) shows the fluid velocity in $v$ direction. The velocity of fluid changes is increased up to 23.26 cm/s in the forward direction and reduced up to 24.53 cm/s in reversed direction. Figure 4.16 (c) shows that there is no change in $w$ direction.  Figure 4.16(d) is visual representation of pressure distribution

50

around the turbine. The maximum pressure of 24.95 Pascals can be seen in the front face of the turbine.
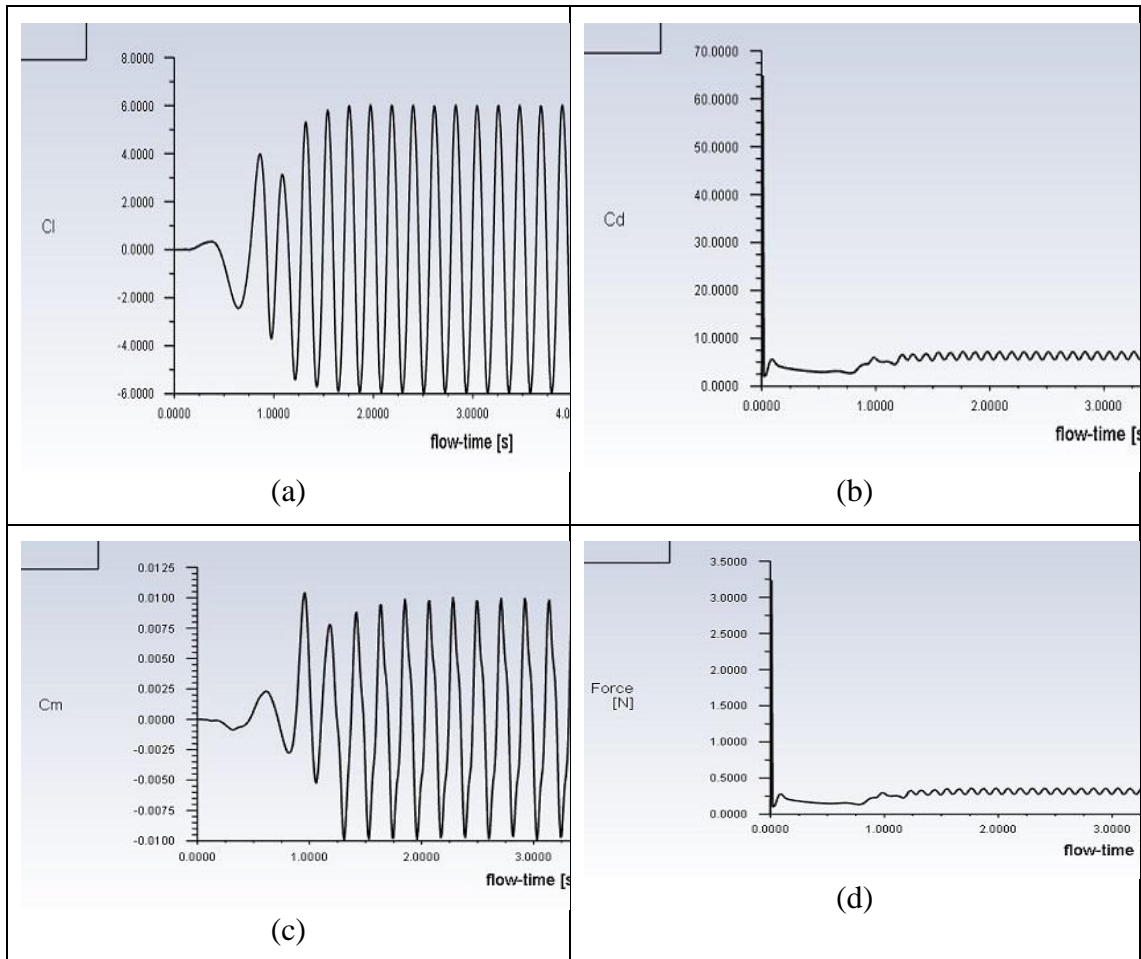


Figure 5.17: (a) coefficient of lift, (b) coefficient of drag, (c) coefficient of momentum, (d) force plot for turbine of 10mm diameter and 19.8cm/s velocity

The simulation result of turbine of diameter 10 mm diameter shows that there is oscillatory motion of the turbine at a low flow velocity of 19.8 cm/s. This shows that there is a periodic hydrodynamic force acting on the turbine which can be harnessed by a suitable power take off mechanism. The periodic motion is seen on the figure 4.17 (c) where the plot of momentum is depicted. The time period of one complete oscillation was measured from the graphical method and the average time period of one complete oscillation is measured to be 0.31 second measured from the graph. Hence, the oscillation frequency or the resonance frequency of the turbine is found to be 3.23 Hz.

Figure 4.17 (a) Shows that there is a periodic change in coefficient of lift from positive to negative values. This means that the force is changing directions in a periodic manner which is the base for Vortex Induced Vibrations. The flow of fluid is directly facing the

turbine so there is a drag force associated with it. But compared to lift force drag force is constant and it shows miniscule oscillation motion. The drag coefficient was found to be averaging on 5 as shown in figure 4.17 (b). The force of drag is around 0.25 newton on the turbine shown in figure 4.17 (d).

### 4.2.6    Turbine diameter 14mm flow velocity 19.8cm/s

From figure 4.18, for a bluff cylinder of diameter 8mm and flow velocity of 19.8 cm/s vertex shedding phenomenon is present. The free stream velocity is 19.8 cm/s and it is seen that there is a velocity increment up to 35.00 cm/s since there is flow around the curvature of the bluff body. It is seen from the figure 4.18 that there is a periodic shedding of vortex around the bluff body. This periodic change in velocity induces lift forces and drag force as well. These periodic forces the body to swing periodically and it reaches the resonance frequency of the turbine.

In the simulation, the oscillation frequency was obtained to be **2.83 Hz**.

From equation (1),

Putting the value of

> Strouhal Number ($S$) = 0.2,

> Freestream velocity of fluid ($U$) = 9.24cm/s,
> Diameter of cylinder ($D$) = 10mm,

The Frequency of oscillation of the cylinder , $f_s = 2.83$ **Hz**.

This shows some strong correlation of simulation results with theoretical research.



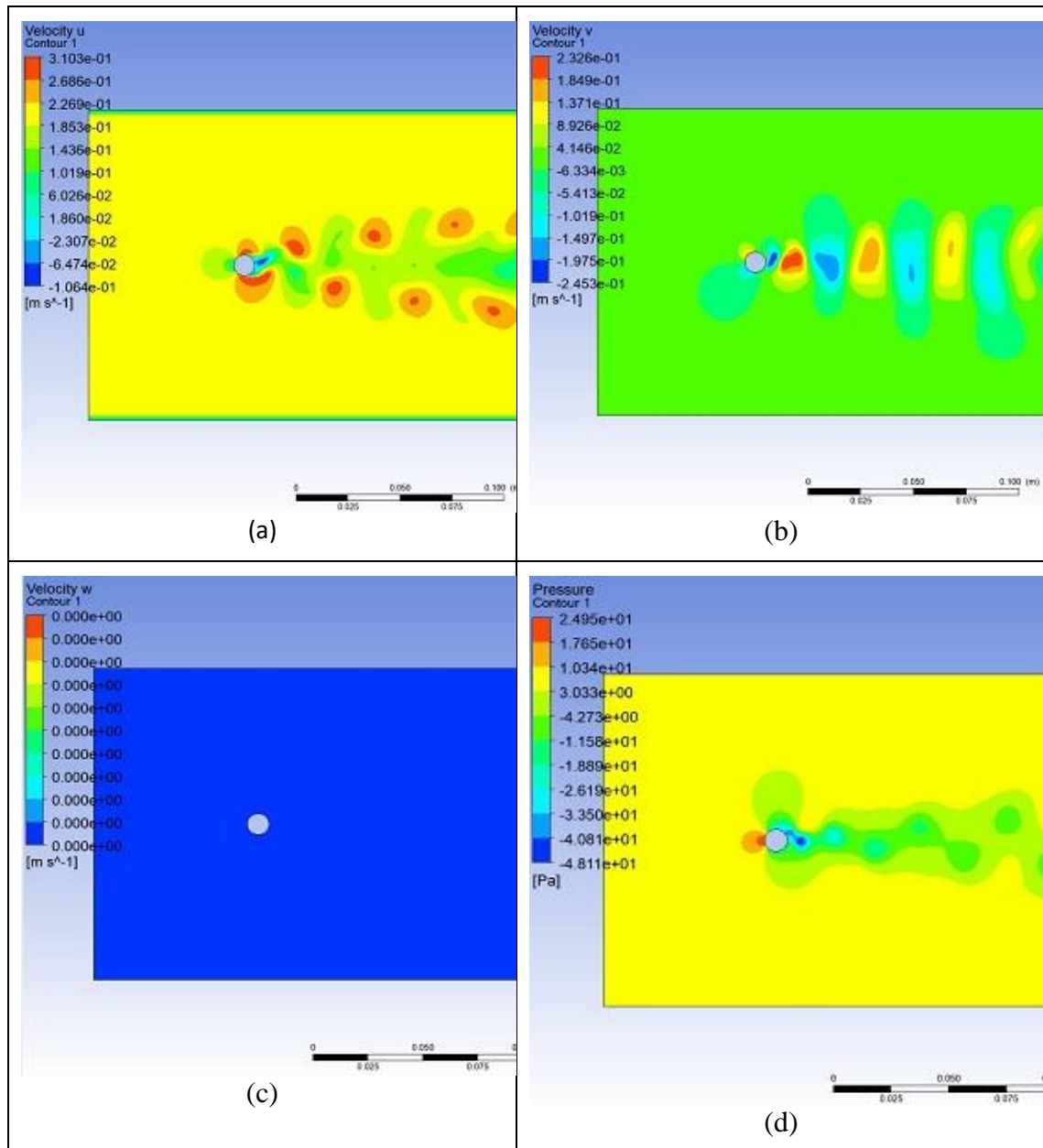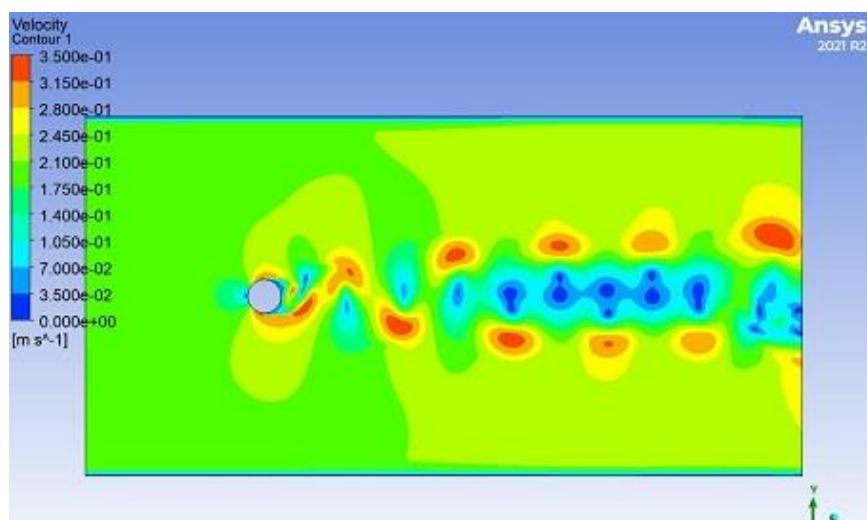Figure 5.18: Vortex shedding in turbine of diameter 14mm at flow velocity 19.8cm/s
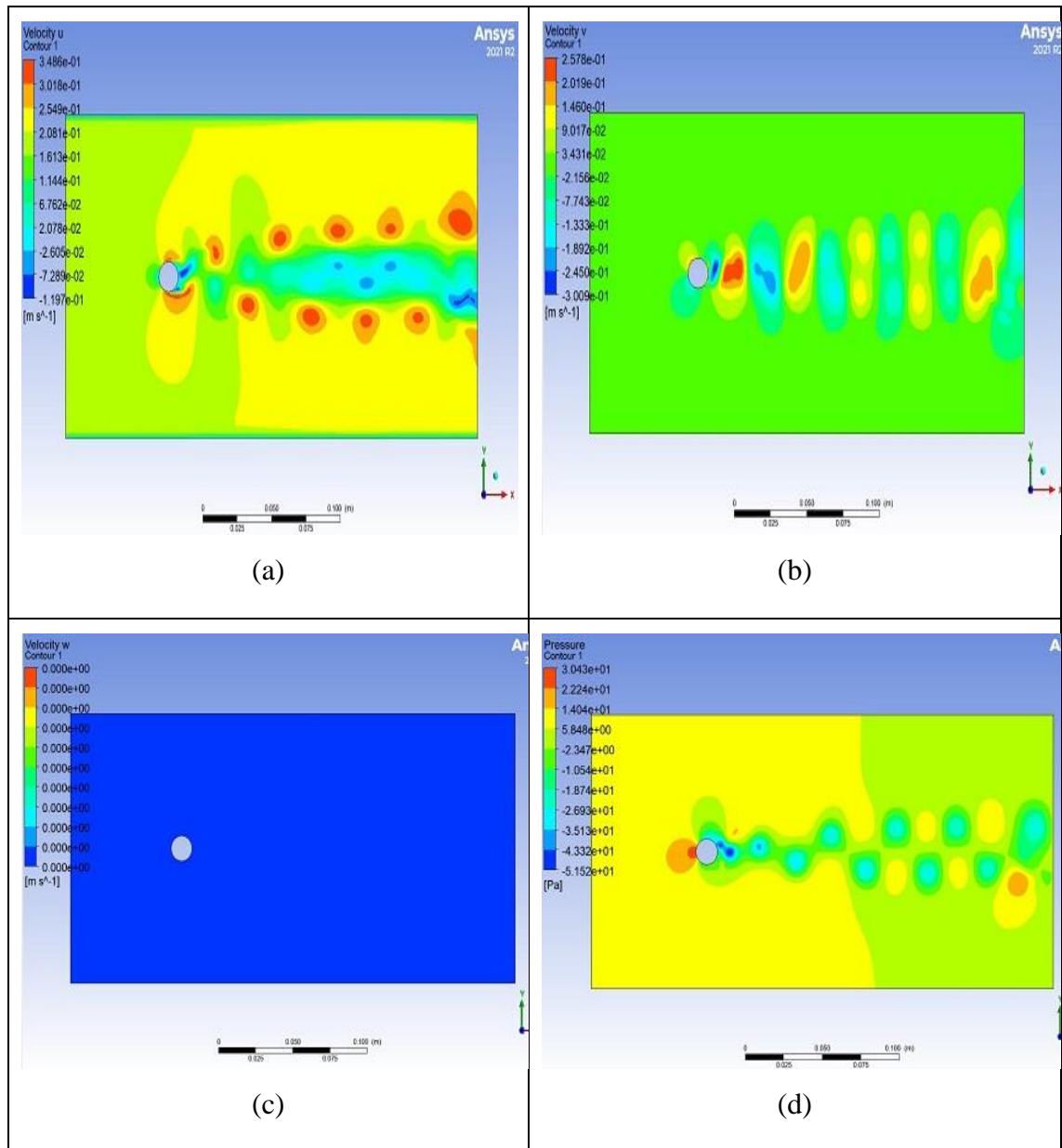
Figure 5.19: (a) Velocity contour in x- axis only, (b) velocity counter in y- axis only, (c) velocity contour in z- axis only, (d) pressure distribution around the mast

The velocity contour of the turbine of 14 mm diameter in the flow velocity of 19.8 cm/s has been divided into respective three-dimensional axes. This shows that the fluid has a changing velocity in two spatial dimensions u and v out of three spatial dimensions (*u, v, w*). Figure 4.19 (a) shows the change in fluid velocity in *u* direction. The velocity of the fluid is increased up to 34.86 cm/s in the forward direction and reduced up to 11.97 cm/s in the reversed direction. Figure 4.19 (b) shows the fluid velocity in *v* direction. The velocity of fluid changes is increased up to 25.78 m/s in the forward direction and reduced up to 30.09 cm/s in reversed direction. Figure 4.19 (c) shows that there is no change in *w* direction. Figure 4.19 (d) is visual representation of pressure distribution around the

53

turbine. The maximum pressure of 30.43 Pascals can be seen in the front face of the turbine
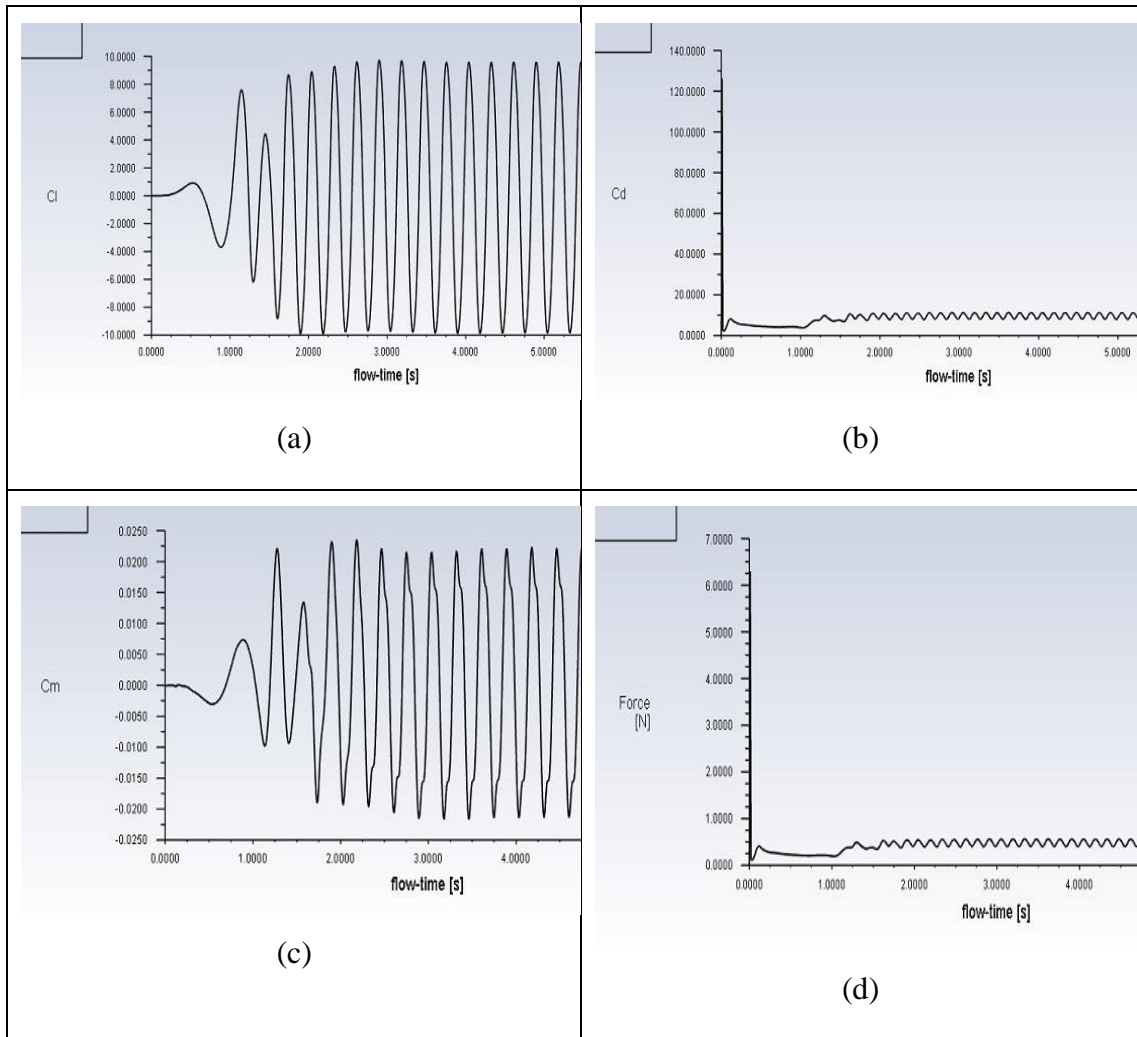


Figure 5.20: (a) coefficient of lift, (b) coefficient of drag, (c) coefficient of momentum, (d) force plot for turbine of 14mm diameter and 19.8cm/s velocity

The simulation result of turbine of diameter 14 mm diameter shows that there is oscillatory motion of the turbine at a low flow velocity of 19.8 cm/s. This shows that there is a periodic hydrodynamic force acting on the turbine which can be harnessed by a suitable power take off mechanism. The periodic motion is seen on the figure 4.20 (c) where the plot of momentum is depicted. The time period of one complete oscillation was measured from the graphical method and the average time period of one complete oscillation is measured to be 0.353 second measured from the graph. Hence, the oscillation frequency or the resonance frequency of the turbine is found to be 2.83 Hz. Figure 4.20 (a) Shows that there is a periodic change in coefficient of lift from positive to negative values. This means that the force is changing directions in a periodic manner

which is the base for Vortex Induced Vibrations. The flow of fluid is directly facing the turbine so there is a drag force associated with it. But compared to lift force drag force is constant and it shows miniscule oscillation motion. The drag coefficient was found to be
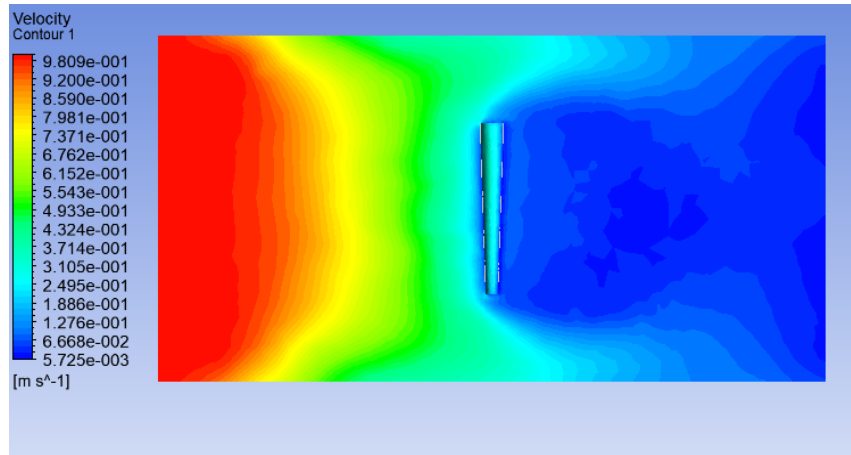


Figure 5.21: velocity contour around the VIV turbine at flow velocity 9.24 cm/s averaging on 10 as shown in figure 4.20 (b). The force of drag is around 0.5 newton on the turbine shown in figure 4.20(d). Figure 14.21 shows the pressure distribution around the turbine in length wise axis.

## 4.3    Analysis of data obtained from CFD simulation

From the analysis of data, we find that there is certain degree of correlation of experimental data with simulation result,

Table 5.11: Experimental data vs Simulated

| Actual data Flow velocity = 9.24cm/s | | | Simulated data Flow velocity = 9.24cm/s | | |
|---|---|---|---|---|---|
| diameter of cylinder (mm) | Average time taken for one oscillation(s) | Frequency of oscillation (Hz) | diameter of cylinder (mm) | Average time taken for one oscillation(s) | Frequency of oscillation (Hz) |
| 8 | 0.38 | 2.63 | 8 | 0.348 | 2.87 |
| 10 | 0.4 | 2.5 | 10 | 0.435 | 2.3 |
| 14 | 0.8 | 1.25 | 14 | 0.555 | 1.8 |

| Actual data Flow velocity = 19.8cm/s | | | Simulated data Flow velocity = 19.8cm/s | | |
|---|---|---|---|---|---|
| diameter of cylinder (mm) | Average time taken for one oscillation(s) | Frequency of oscillation (Hz) | diameter of cylinder (mm) | Average time taken for one oscillation(s) | Frequency of oscillation (Hz) |
| 8 | 0.29 | 3.45 | 8 | 0.294 | 3.4 |
| 10 | 0.38 | 2.63 | 10 | 0.31 | 3.23 |
| 14 | 0.48 | 2.08 | 14 | 0.353 | 2.83 |

Figure 4.22 and 4.23correlation shows that the experimental data can be verified with the simulation results.
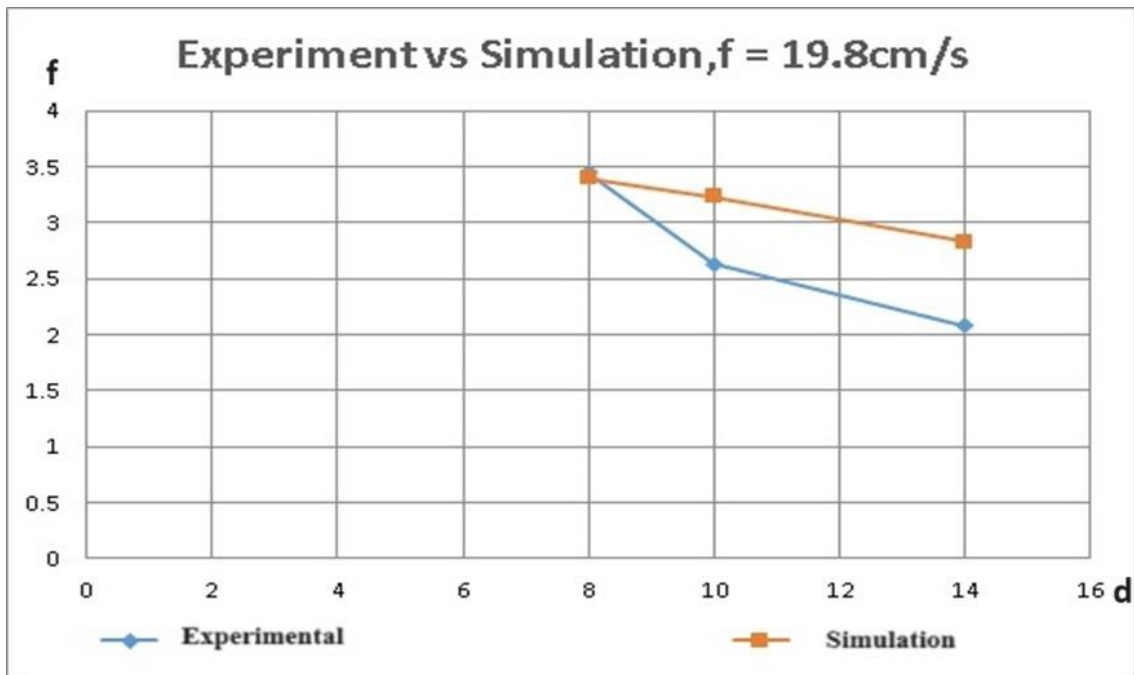


Figure 5.22: Graphical representation of experimental vs simulation data for flow velocity 19.8 cm/s
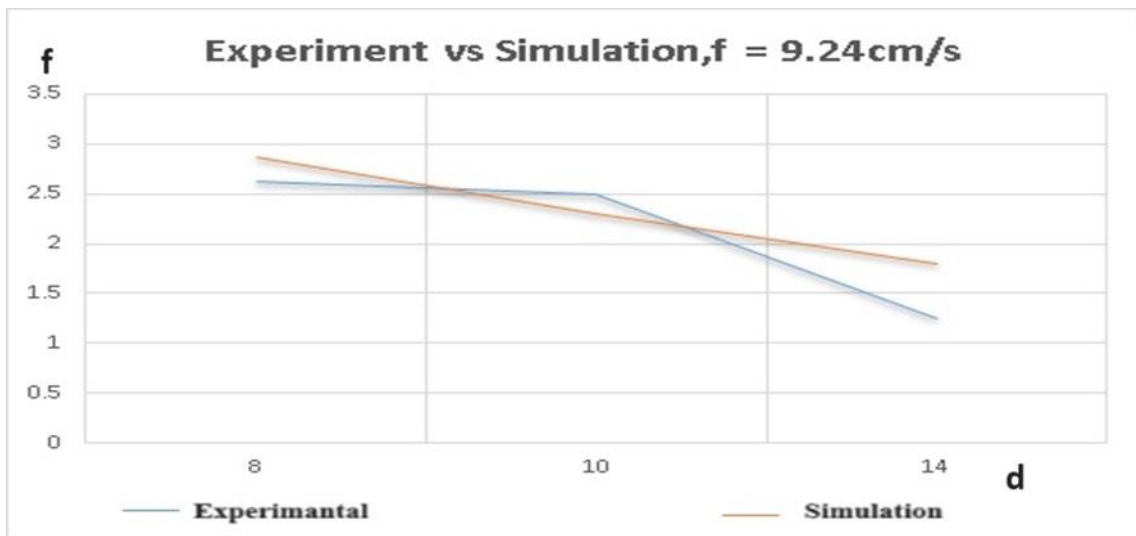


Figure 5.23: Graphical representation of experimental vs simulation data for flow velocity 9.24 cm/s

Table 5.12: Deviation error percentage

| Flow velocity = 9.24cm/s | | |
|---|---|---|
| Frequency of oscillation (Hz) (Experimental) | Frequency of oscillation (Hz) (Simulation) | % Error |
| 2.63 | 2.87 | 0.091255 |
| 2.5 | 2.3 | 0.08 |
| 1.25 | 1.8 | 0.44 |
| Flow velocity = 19.8cm/s | | |
| Frequency of oscillation (Hz) (Experimental) | Frequency of oscillation (Hz) (Simulation) | % Error |
| 3.45 | 3.4 | 0.014493 |
| 2.63 | 3.23 | 0.228137 |
| 2.08 | 2.83 | 0.360577 |

From table 4.12, it is clear that there is very minute error when the experimental and simulation data are compared. The error percentage is calculated as following:

$$\% \ error \ = \frac{|(Experimental \ Data - Simulation \ Data)|}{Experimental \ Data} \qquad (12)$$

As the data have slight margin of error, we can rely on simulation for verification of different models of turbines rather than experimental data since they are costly and time consuming. Scaling up is also easier in simulation and tweaking the parameters can also be done in an instant.

# CHAPTER FIVE: CONCLUSION AND RECOMMENDATION

## 5.1 Conclusions

The experiment and simulations were performed successfully and the outcomes of the results shows a promising result on extraction of renewable energy from slow flowing water currents. The results shows that a significant amount of energy can be extracted from a low flowing water currents by extracting energy from the vortex induced vibration-based turbines. The experiments showed that at a flow velocity of 9.24 cm/s, model turbine having length 100 mm, diameter of 8 mm, 10 mm & 14 mm can extract a power of 2.92 mW, 4.05 mW, 1.89 mW respectively. Whereas for a flow velocity of 19.8 cm/s, model turbine having length 100 mm, diameter of 8 mm, 10 mm & 14 mm can extract a power of 4.49 mW, 5.18 mW, 4.63 mW respectively. This shows that there is an efficient shape of turbine for a particular flow velocity at which the power extraction is maximum.The prototype model could only produce a small fraction of power but if the device is scaled up and large group of turbines are placed in an area a large amount of renewable energy can be harvested. This device produces renewable clean energy which will be helpful for providing clean energy sources. As, there are losses involved in the actual system the power produced is less compared to the theoretical value. Because of simplicity of design the turbine costs less and is best solution for energy extraction from low flowing currents. The cost of the system is minimum and its maintenance is also negligible which make this turbine viable solution for under slow flowing water and marine clean energy extraction.

## 5.2 Recommendations

After successfully completion of both the experiments and simulation the following recommendations are done which may help better understanding of the present research,

- Use of various materials like aluminum, steel, wood etc.
- Used of springs made of different materials.
- Use of different fluids with different density e.g., clean water and salty ocean water.
- Fluid simulating in 3-D space.

## 5.3 **Future works**

This work can be further refined the following works are done:

- A suitable test facility with variable flow velocity can outcome more precise data and more in-depth research.
- Use of modern sensing technologies like microcontrollers and position sensors can be used to more accurately measure the displacement and oscillation frequency as well as power produced.
- Perform simulation and experiments with different shapes and sizes as well as material.

Following works will be done to further expand this thesis research,

- A real size model will be developed to actually produce electrical energy and measure its viability.
- The prototype will be used in various locations and flow velocities to effectively study its efficiency.
- More efficient turbines will be developed studying the previous models.
- The turbines will be used to extract energy from marine and slow flowing river currents.
- The feasibility of the turbines will be studied for the production of green hydrogen.

# REFERENCES

1. Ian Tiseo,2023, *Annual global emissions of carbon dioxide 1940-2022*, https://www.statista.com/statistics/264699/worldwide-co2-emissions/#:~:text=The%20carbon%20dioxide%20emissions%20released,billion%20metric%20tons%20of%20CO%E2%82%82

2. Bobby Zarubin, 2015, *Ocean Current Energy: Underwater Turbines* , Submitted as coursework for PH240, Stanford University, Fall 2014

3. bp *Statistical Review of World Energy 2022 | 71st edition*, https://www.bp.com/content/dam/bp/business-sites/en/global/corporate/pdfs/energy-economics/statistical-review/bp-stats-review-2022-full-report.pdf

4. S. M. Ingole, Dr. S. S. Patil, 2021 *DESIGN AND FINITE ELEMENT ANALYSIS OF VORTEX INDUCED VIBRATION (VIV) SYSTEM,* 2021 IJCRT | Volume 9, Issue 3 March 2021 | ISSN: 2320-2882

5. Ajay Kaviti and Amit Thakur. *Power Generation from Wind Using Bladeless Turbine*, pages 139–146. 08 2021.

6. UN,2015, *Sustainable Development Goals*, https://sdgs.un.org/goals

7. (Watkins, S. ,2010, Aerodynamic noise and its refinement in vehicles. Vehicle Noise and Vibration Refinement, 219–234. doi:10.1533/9781845698041.3.219)

8. dnrc.mt.gov , Stream Discharge using the Float-Area Method, https://dnrc.mt.gov/_docs/water/Float_area_method.pdf

9. Yousef Abdulbari Atfah Sharul Sham Dol Mohammed Alavi Catherine Kamal Samy, Hamza Ben Ahmadi. *Design of portable vortex bladeless wind turbine: The preliminary study.* Journal of Advanced Research in Applied Mechanics, 2023.

10. Michelle Fogarty Levi Kilcher and Michael Lawson. *Marine energy in the united states: An overview of opportunities.* 2021.

11. Unhale SG Nirmal RS Chaudhari CC, Shriram MA. *Fabrication of vortex bladeless windmill power generation model*. Int J Sci Technol Eng 3(12):52–56, 2017.

12. M. Meshram A.P. Qamar M., Verma and N. Isaac. *Model studies for desilting basin for teestavi h.e. project, sikkim – a case study*. 9th IAHR International Symposium

on Hydraulic Structures (9th ISHS)(DOI: 10.26077/9da6-8da5) (ISBN 978-1-958416-07-5), 2022.

13. Arnold L. Gordon and Claudia. Cenedese. *ocean current*, chapter https://www.britannica.com/science/ocean-current. Encyclopedia Britannica, 2023.

14. Am. J. Phys 1977. *Life in the low-Reynolds number world*, chapter 5. Nelson – Biological Physics, 1977.

15. Vinoth Babu N Balakrishnan S P, Arun R. *Design, analysis and prototype of vortex bladeless wind turbine*. International Research Journal of Engineering and Technology (IRJET) e-ISSN: 2395-0056 p-ISSN: 2395-0072, 2019.

16. Varun Michael Lobo. *Design of a vortex induced vibration based marine hydro-kinetic energy system*,2012

17. Bearman, Peter W. "Vortex shedding from oscillating bluff bodies." Annual review of fluid mechanics 16.1 (1984): 195-222.

18. Zhang, W., Li, X., Ye, Z., & Jiang, Y. (2015). Mechanism of frequency lock-in in vortex-induced vibrations at low Reynolds numbers. Journal of Fluid Mechanics, 783, 72-102. doi:10.1017/jfm.2015.548

19. Mawat, Mohammed. (2018). Simulation of Cylindrical Body Structure Subjected to Flow in Different Reynolds Number Regimes. Muthanna Journal of Engineering and Technology. 6. 45-51. 10.18081/mjet/2018-6/45-51.

20. Williamson, Charles HK, and R. Govardhan. "Vortex-induced vibrations." Annu. Rev. Fluid Mech. 36 (2004): 413-455.

Figure A: (a) Experiment conducted on Bhot khola river stream, Gorkha, Nepal. (b) Bhot khola site view, (c) Measurement of displacement, (d) Experimental tank

Figure B: View of experimental tank from another side



Figure C: Top view of experimental tank showing turbine and measurement scale

# Thesis

SIMILARITY INDEX **12**%

PRIMARY SOURCES

**1** elibrary.tucl.edu.np:8080 Internet
310 words — **2%**

**2** scholarsmine.mst.edu Internet
230 words — **1%**

**3** Krzysztof Brzostowski. "Toward the Unaided Estimation of Human Walking Speed Based on Sparse Modeling", IEEE Transactions on Instrumentation and Measurement, 2018
Crossref
192 words — **1%**

**4** link.springer.com Internet
92 words — **1%**

**5** elibrary.tucl.edu.np Internet
87 words — **1%**

**6** Hosseini, Maryam Sadat. "On the Mechanics of Non-Interlocking and Interlocking Patterned Interfaces Inspired by Nature", Purdue University, 2023
ProQuest
72 words — **< 1%**

**7** escholarship.org Internet       50 words — $< 1\%$

**8** Gao, Linyue. "Experimental Investigations onWind Turbine Icing Physics and Anti-/De-icing   48 words — $< 1\%$   Technology.", Iowa State University
ProQuest

**9** Darwish, Ahmed Abdelazim Ahmed.      47 words — $< 1\%$
"Comparative Microstructure Evaluation of Nickel and Iron Alloys Under Fretting Wear for Applications in Advanced Reactors.", North Carolina State University, 2021
ProQuest

**10** large.stanford.edu
Internet      44 words — $< 1\%$

**11** mech.pcampus.edu.np
Internet      42 words — $< 1\%$

**12** www.un.org
Internet      33 words — $< 1\%$

**13** www.statista.com
Internet      32 words — $< 1\%$

**14** Yiben Gao, Yi-Ning Wang, Weiyi Li, Chuyang Y.   27 words — $< 1\%$   Tang. "Characterization of internal and external concentration polarizations during forward osmosis processes", Desalination, 2014
Crossref

15 Hung, Tien-C. "Biomimetic Solid/Fluid Separation: 26 words — < 1% Theory and Application", Proquest, 2014.
ProQuest

16 dspace.unza.zm Internet 26 words — < 1%

17 Alireza Modir, Mohsen Kahrom, AnoshirvanFarshidianfar. "Mass ratio effect on vortex 25 words — < 1% induced vibration of a flexibly mounted circular cylinder, an experimental study", International Journal of Marine Energy, 2016
Crossref

18 culmimg.pw
Internet 24 words — < 1%

19 Ultrasonography in Vascular Diagnosis, 2011.
Crossref 20 words — < 1%

20 hdl.handle.net
Internet 18 words — < 1%

21 scholarworks.uno.edu
Internet 18 words — < 1%

22 api.research-repository.uwa.edu.au
Internet 17 words — < 1%

23 www.irjmets.com
Internet 14 words — < 1%

24 H. R. Brown, O. B. Ilyinsky. "The ampullae of Lorenzini in the magnetic field", Journal of Comparative Physiology ? A, 1978
Crossref

12 words — < 1%

25 dokumen.pub
Internet

12 words — < 1%

26 Wang, Yanming. "Atomistic and Phase Field Models of Catalyzed Nanowire Growth.", Stanford University, 2020
ProQuest

11 words — < 1%

27 arxiv.org
Internet

11 words — < 1%

dspace.alquds.edu
28 Internet

11 words — < 1%

29 dspace.iiuc.ac.bd:8080
Internet

11 words — < 1%

30 ethesisarchive.library.tu.ac.th
Internet

11 words — < 1%

31 core.ac.uk
Internet

10 words — < 1%

32 dev.physicslab.org
Internet

10 words — < 1%

| 33 | inis.iaea.org | 10 words — < 1% |
| --- | --- | --- |
| | Internet | |

| 34 | mobt3ath.com | 10 words — < 1% |
| --- | --- | --- |
| | Internet | |

| 35 | ujcontent.uj.ac.za | 10 words — < 1% |
| --- | --- | --- |
| | Internet | |

| 36 | www.nyserda.ny.gov | 10 words — < 1% |
| --- | --- | --- |
| | Internet | |

37  Alireza Modir, Navid Goudarzi. "Experimental investigation of Reynolds number and spring stiffness effects on vortex induced vibrations of a cylinder", European Journal of Mechanics - B/Flui
Crossref

9 words — < 1%
rigid circular ds, 019

38  Brandao, Filipe Leite. "Numerical Modeling andSimulation of Cavitating Flows in

Different    9 words — < 1%

Regimes", University of Minnesota, 2023
ProQuest

39  Leontini, J.S.. "Predicting vortex-induced vibrationfrom driven oscillation results",

Applied    9 words — < 1%

Mathematical Modelling, 200610
Crossref

**40**

Rubol, S., A. Freixa, A. Carles-Brangarí, D. Fernàndez-Garcia, A.M. Romaní, and X. SanchezVila. "Connecting bacterial colonization to physical and biochemical changes in a sand box infiltration experiment", Journal of Hydrology, 2014.
Crossref

9 words — < 1%

**41**

Vispute, Dhwanit. "Inter and Intra-Subject Variations in Alignment Between the Bones of the Hindfoot in Bilateral Standing for the Normal Population", Drexel University, 2020
ProQuest

9 words — < 1%

**42** aip.scitation.org
Internet

9 words — < 1%

**43** eprints.utar.edu.my
Internet

9 words — < 1%

**44** www.iaee.org
Internet

9 words — < 1%

**45** www.intechopen.com
Internet

9 words — < 1%

**46**

"Recent Trends in Thermal Engineering", Springer Science and Business Media LLC, 2022
Crossref

8 words — < 1%

**47** Aimeé González-Suárez, Pamela Guerra-Blanco,Tatyana Poznyak, Javier Morales, Isaac Chairez,

8 words — < 1%

Jaime Dueñas-Moreno. "Experimental criteria of sequential

continuous ozonation and semi-continuous biodegradation for the decomposition of 4-chlorophenol", Journal of Environmental Chemical Engineering, 2023
Crossref

48
Higgs, Zachary C.. "Analyzing Temporal Interference for Use with Dual Site Transcranial Magnetic Stimulation", Iowa State University, 2023
ProQuest

8 words — < 1%

49
Lei Zheng, William E. Price, James McDonald, Stuart J. Khan, Takahiro Fujioka, Long D. Nghiem. "New insights into the relationship between draw solution chemistry and trace organic rejection by forward osmosis", Journal of Membrane Science, 2019
Crossref

8 words — < 1%

50
Nixon, Mark S., and Alberto S. Aguado. "Low-level 8 words — < 1% feature extraction (including edge detection)", Feature Extraction and Image Processing, 2002.
Crossref

51  nec.edu.np
Internet

8 words — < 1%

52  nepalindata.com
Internet

8 words — < 1%

53  ppgen.poli.usp.br
Internet

8 words — < 1%

54  su-plus.strathmore.edu
Internet

8 words — < 1%

70

**55** www.europarl.europa.eu
Internet

8 words — < 1%

www.mdpi.com

**56** Internet

8 words — < 1%

**57** ynu.repo.nii.ac.jp Internet

8 words — < 1%

**58** Phogole, Bopaki Testimonies. "An Evaluation of theEffectiveness of Interventions to

Transition Low-          7 words — < 1%

Income Households Towards the Adoption of Cleaner Energy
Sources on the Mpumalanga Highveld", University of
Johannesburg (South Africa), 2023
ProQuest

EXCLUDE QUOTES            ON                      EXCLUDE SOURCES        < 6 WORDS
EXCLUDE BIBLIOGRAPHY ON                           EXCLUDE MATCHES        OFF